Molecular Therapy
Nucleic Acids
Original Article

Targeting the *IGF1R* Pathway in Breast Cancer Using Antisense lncRNA-Mediated Promoter *cis* Competition

Lingling Pian,[1] Xue Wen,[1] Lihua Kang,[1] Zhaozhi Li,[1] Yuanyuan Nie,[1] Zhonghua Du,[1,2] Dehai Yu,[1,2] Lei Zhou,[1] Lin Jia,[1,2] Naifei Chen,[1,2] Dan Li,[1,2] Songling Zhang,[1,3] Wei Li,[1,3] Andrew R. Hoffman,[2,3] Jingnan Sun,[1,3] Jiuwei Cui,[1,3] and Ji-Fan Hu[1,2,3]

[1]Stem Cell and Cancer Center, First Affiliated Hospital, Jilin University, Changchun, Jilin 130061, PRC; [2]Stanford University School of Medicine, VA Palo Alto Health Care System, Palo Alto, CA 94304, USA

Aberrant insulin-like growth factor I receptor (IGF1R) signaling pathway serves as a well-established target for cancer drug therapy. The intragenic antisense long noncoding RNA (lncRNA) IRAIN, a putative tumor suppressor, is downregulated in breast cancer cells, while IGF1R is overexpressed, leading to an abnormal IGF1R/IRAIN ratio that promotes tumor growth. To precisely target this pathway, we developed an "antisense lncRNA-mediated intragenic *cis* competition" (ALIC) approach to therapeutically correct the elevated IGF1R/IRAIN bias in breast cancer cells. We used CRISPR-Cas9 gene editing to target the weak promoter of IRAIN antisense lncRNA and showed that in targeted clones, intragenic activation of the antisense lncRNA potently competed in *cis* with the promoter of the IGF1R sense mRNA. Notably, the normalization of IGF1R/IRAIN transcription inhibited the IGF1R signaling pathway in breast cancer cells, decreasing cell proliferation, tumor sphere formation, migration, and invasion. Using "nuclear RNA reverse transcription-associated trap" sequencing, we uncovered an IRAIN lncRNA-specific interactome containing gene targets involved in cell metastasis, signaling pathways, and cell immortalization. These data suggest that aberrantly upregulated IGF1R in breast cancer cells can be precisely targeted by *cis* transcription competition, thus providing a useful strategy to target disease genes in the development of novel precision medicine therapies.

INTRODUCTION

The insulin-like growth factor (IGF) signaling axis plays a critical role in development, growth, and maintenance of many tissues.[1,2] The mitogenic ligands IGF-I and IGF-II interact with the cell membrane IGF-I receptor (*IGF1R*), which belongs to the tyrosine kinase receptor family. Increased activity of the IGF axis has long been recognized as a critical factor in tumor growth and progression.[3–5] *IGF1R* is dysregulated in a variety of human malignancies, including breast cancer.[6–8] Activation of this pathway leads to stimulation of downstream mitogen-activated protein kinase (MAPK) and/or phosphatidylinositol 3-kinase (PI3K)/protein kinase B (AKT) signaling cascades,[9] resulting in increases in cell proliferation, antiapoptosis, and drug resistance through autocrine, paracrine, and endocrine pathways.[10–13] As a result, *IGF1R* has been recognized as a promising target for the development of precision tumor therapy.[14,15]

In the past decade, numerous extensive cancer trials have been performed using a variety of agents that are specifically directed against the *IGF1R* signaling pathway.[16–18] Unfortunately, the vast majority of therapies using monoclonal antibodies and tyrosine kinase inhibitors to target *IGF1R* failed in late clinical trials.[17,19] Thus, other novel approaches are urgently needed to target this pathway in tumors.

Approximately 50% of breast tumors show increased transcription of *IGF1R*,[14] but little is known about how *IGFIR* becomes dysregulated in tumors. Using a novel R3C (RNA-guided chromatin conformation capture) method, we recently identified *IRAIN*, an intragenic antisense long noncoding RNA (lncRNA), that arises within the *IGF1R* promoter complex.[20] *IRAIN* was expressed in a monoallelic manner, with the expression of the lncRNA exclusively from the paternal chromosome, and it appeared to serve as a tumor suppressor in hematopoietic tumors[20]. *IRAIN* was also aberrantly regulated in breast cancer, exhibiting a pattern of allele-switch: the allele expressed in normal tissues was suppressed, while the normally silenced allele was expressed.[21] Recent studies have shown that this lncRNA is also dysregulated in non-small-cell lung cancer[22] and pancreatic cancer.[23]

Received 21 February 2018; accepted 27 April 2018;
https://doi.org/10.1016/j.omtn.2018.04.013.

[3]These authors contributed equally to this work.

Correspondence: Ji-Fan Hu, MD, PhD, Cancer Center, First Hospital, Jilin University, Changchun 130021, PRC.
E-mail: jifan@stanford.edu
Correspondence: Jiuwei Cui, Cancer Center, First Hospital, Jilin University, Changchun 130021, PRC.
E-mail: cuijiuwei@jlu.edu.cn

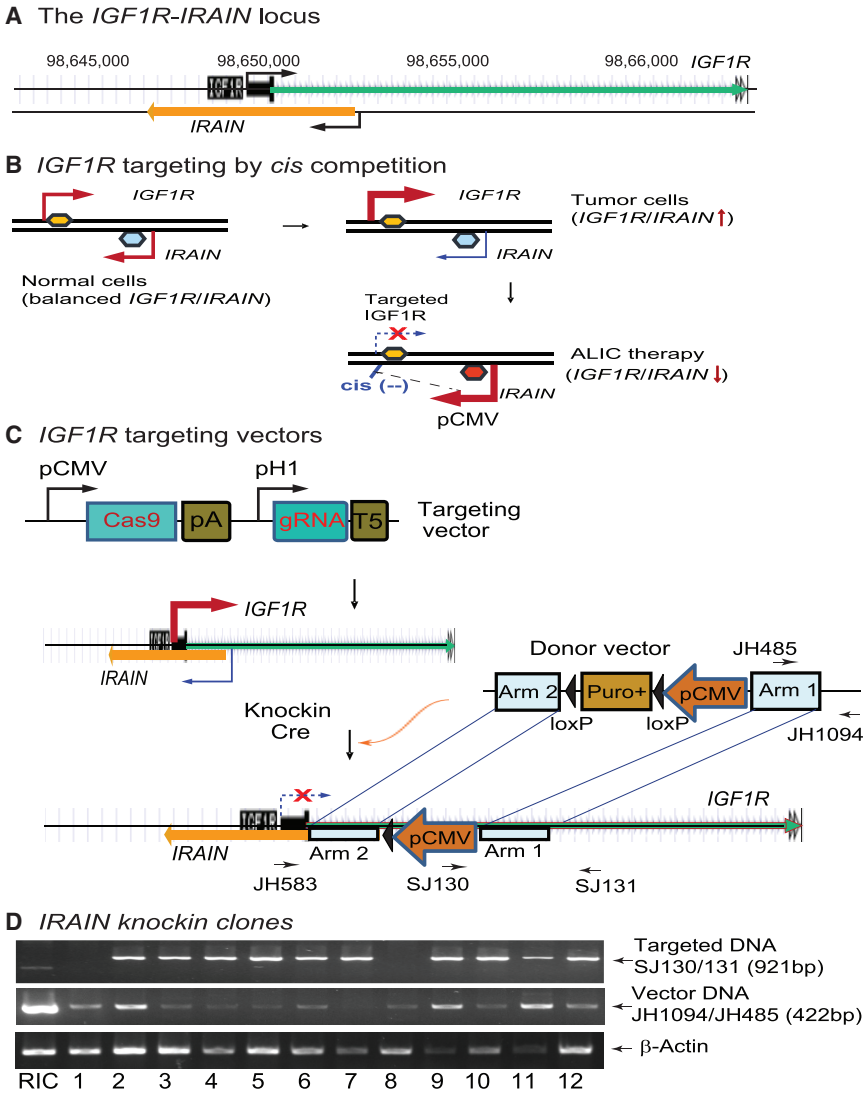

Figure 1. Targeting the *IGF1R* Pathway by Antisense lncRNA *IRAIN*-Mediated *cis* Competition

(A) The orientation of *IGF1R* and *IRAIN*. The antisense *IRAIN* lncRNA is transcribed from an intronic promoter of the *IGF1R* gene. (B) Schematic diagram of the antisense lncRNA-mediated *cis* competition in the *IGF1R* signaling pathway. In normal tissues, the transcription of the *IGF1R*/*IRAIN* locus is balanced. In breast cancer cells, however, *IGF1R* is upregulated while *IRAIN* is downregulated. This unbalanced expression leads to increased activation of the *IGF1R* signaling pathway. An ALIC targeting approach is used to reverse this unbalance. A strong CMV promoter is inserted in front of the *IRAIN* lncRNA to induce increased production of *IRAIN*, which then competes in *cis* with the overlapping *IGF1R* promoter and dampens the *IGF1R* signaling pathway in tumor cells. This provides a molecular basis for the development of the precision therapy against breast cancer. (C) ALIC targeting of *IGF1R* by CRISPR Cas9-guided recombinant knockin. Cas9, CRISPR Cas9; gRNA, Cas9 guiding RNA; pCMV, CMV promoter; pH1, RNA polymerase III H1 promoter; Cre, Cre recombinase; pA, SV40 poly(A) signal; loxP, the locus of X-over P1 recombination site recognized by Cre; Arm 1-2, the genomic sequences used for recombination. Under the guidance of gRNAs, Cas9-mediated genomic recombination at the *IRAIN* locus, resulting in the insertion of the CMV promoter-puro cassette in front of the *IRAIN*. After puromycin selection, the cells were treated with Cre to remove the selection marker Puro$^+$. In the selected cell clones, *IRAIN* is under the control of the strong promoter pCMV. The upregulated transcription of this antisense lncRNA will compete in *cis* with that of the sense *IGF1R* mRNA. (D) Initial screening of targeted cell clones by PCR. Primers were designed from the *IRAIN* arm, selection marker, and vector sequences. PCR was used to identify the wild-type, targeted DNA, and vector DNAs. RIC, control cells that were generated in parallel with ALIC targeting by transfecting the cells with only the donor vector DNA and selected with puromycin. As the control, RIC cells carry the randomly inserted donor vector DNA. Clones 1–12, cell clones that were generated by co-transfection with Cas9 target vector-donor vector DNAs and selected by both puromycin and ganciclovir. Targeting cell clones not only carry the *IGF1R* targeting allele, but also contain some amount of the randomly inserted donor vector DNA in the genome. Among them, clone 7 contains a minimum amount of randomly inserted vector DNA and was thus used for subsequent studies.

IRAIN is transcribed in an antisense orientation using a promoter located in intron 1 of *IGF1R*. By overlapping with the *IGF1R* promoter in antisense, *IRAIN* lncRNA directly competes with *IGF1R* in *cis* for transcriptional machinery.[20] In cancer cells, however, *IRAIN* is downregulated, and the decrease in this *cis* competition control leads to upregulation of *IGF1R*, increasing the activation of the IGF signaling pathway.[20,21] In this communication, we attempted to target the *IGF1R* pathway in tumors by increasing the transcription of the downregulated *IRAIN* antisense suppressor lncRNA, thereby enhancing the *cis* competition mechanism. The rebalanced production of the oncogenic *IGF1R* and tumor suppressor *IRAIN* should decrease the signaling cascades that stimulate the growth of breast cancer cells.

RESULTS

Targeted Activation of IRAIN Antisense Tumor Suppressor lncRNA

IRAIN is transcribed in an antisense direction to *IGF1R* from an intronic promoter (Figure 1A). In normal tissues, expression of the sense *IGF1R* coding mRNA and the antisense *IRAIN* are regulated reciprocally. Breast cancer cells, however, are characterized by upregulated *IGF1R* and downregulated *IRAIN* (Figure 1B, top). The activated *IGF1R* pathway in tumors is associated with tumor growth and metastasis. To precisely target the *IGF1R* pathway, we devised an "antisense tumor suppressor lncRNA-mediated intragenic *cis* competition" (ALIC) approach (Figure 1B, bottom). Specifically, the aberrant *IGF1R* expression in tumors was targeted by increasing the

IRAIN antisense suppressor lncRNA, which competes with the *IGF1R* promoter in *cis*.

As a proof-of-concept study to target the *IGF1R* pathway, we used the CRISPRCas9 gene-editing system to insert a strong cytomegalovirus (CMV) promoter in front of *IRAIN* that would increase the expression of the *IRAIN* lncRNA (Figure 1B). We hypothesized that *IRAIN* competes in *cis* with the overlapping *IGF1R* promoter and thus downregulates the *IGF1R* pathway. We co-transfected the targeting and donor vectors into MDA-MB-231 breast cancer cells (Figure 1C). With the aid of the guide RNAs (gRNAs) (Figure S1), Cas9 induced homologous recombination at the *IRAIN* locus. Puromycin was used to select the positive cells, and ganciclovir was then added to the cell medium to reduce cells that had random integration of the donor vector in the genome. After targeting, *IRAIN* would be under the control of an introduced strong promoter that drives the high expression of the lncRNA that would compete with sense *IGF1R*-coding mRNA (Figure 1C).

After co-transfection with the Cas9 targeting vector and the donor vector, we selected cells using puromycin and ganciclovir. We collected stable cells (clones 1–12) and confirmed the knockin targeting using a series of PCR primers located in the donor vector, arms, and genomic DNAs (Figure 1D). In selected clones, we detected the specific target DNAs (Figure 1D, top), although some cell clones also contained some random insertion of the donor vector (Figure 1D, middle). As a control, MDA-MB-231 cells were transfected with donor vector DNA and were selected with puromycin in parallel with *IGF1R* targeting. As expected, these random insertion cell (RIC) control cells did not carry the targeting DNA sequence. Instead, only the randomly inserted donor vector DNA was detected (Figure 1D, middle, lane 1). Because cell clone 7 contained a minimum amount of randomly inserted vector DNA in the genome, we focused on this clone for the subsequent studies.

Targeted Activation of IRAIN Inhibits IGF1R Expression

To examine the targeting of *IGF1R* by the ALIC approach, we first examined the expression of *IGF1R* and *IRAIN* in selected cell clones. As predicted, *IGF1R* was upregulated and *IRAIN* was downregulated in RIC control cells. In targeted clones, however, we detected a dramatic increase of the *IRAIN* antisense lncRNA, in parallel with a significant downregulation of *IGF1R* (Figure 2A).

The puromycin selection marker was removed from cell clone 7 by transfecting the cells with CMV-Cre-Neo vector DNA. Ultimately, two cell clones were used for subsequent studies (ALIC1, ALIC2). As a control, RIC cells were also treated with CMV promoter (pCMV)-Cre-Neo DNA (CTL1, CTL2). Two ALIC clones showed clear targeting to the *IGF1R* region as compared with the control cells (CTL) (Figure 2B). We amplified the whole targeting region, cloned it into a pJet vector, and performed DNA sequencing for the recombination sites (Figure S2). DNA sequencing confirmed the correct targeting of *IGF1R/IRAIN* by Cas9-mediated homologous recombination.

Using qPCR, we showed that *IRAIN* was increased by ALIC targeting, while *IGF1R* was significantly downregulated in ALIC1-2 cells (Figure 2C), presumably due to the antisense lncRNA *cis* competition. Using western blotting, we confirmed that the *IGF1R* protein was also downregulated in targeted cells (Figure 2D).

Rescue of IGF1R by IRAIN siRNAs in ALIC-Targeted Cells

To further delineate the role of ALIC targeting, we examined whether the *cis* inhibition of *IGF1R* could be rescued by *IRAIN* knockdown using small interfering RNAs (siRNAs). The CMV-*IRAIN* knockin ALIC cells were treated with three *IRAIN* siRNAs and were collected for quantitation of *IGF1R* and *IRAIN*. siRNA treatment decreased *IRAIN* lncRNA in ALIC-targeted cells (Figure S3). As expected, *IGF1R* was inhibited in *cis* by *IRAIN* in scramble control (siCT) control cells (ALIC + siCT). In siRNA-treated cells (ALIC + IRAIN-siRNA [siIRAIN]), however, the siRNA-induced *IRAIN* knockdown partially rescued the downregulated *IGF1R* (Figure 2E). These data suggest the siRNA-induced post-transcriptional knockdown of *IRAIN* lncRNA cannot fully release the *cis* inhibition of *IGF1R*-induced by ALIC targeting.

In a separate study, we also examined whether lentivirus-overexpressed *IRAIN* was able to affect the *IGF1R*. We used a lentivirus to overexpress the *IRAIN* 5K cDNA in MDA-MB-231 tumor cells. The copGFP lentiviral vector was used as the negative control (vector). After selection by puromycin, cells were collected for gene expression analysis. As seen in Figure 2F, tumor cells overexpressed *IRAIN* after lentiviral transfection. However, the *trans* overexpression of *IRAIN* did not reduce the expression of the endogenous *IGF1R* as originally expected. As a matter of fact, the *IGF1R* mRNA was slightly increased in these cells, although the specific mechanism is currently unknown.

Targeted Inhibition of IGF1R Alters the Phenotypes of MDA-MB-231 Tumor Cells

After the ALIC targeting of *IGF1R*, we examined the phenotypes of the MDA-MB-231 breast cancer cells. First, we measured cell proliferation in targeted cells. As shown in Figure 3A, the rebalance of the *IGF1R/IRAIN* ratio was associated with reduced proliferation in two MDA-MB-231 cell clones.

We also examined if ALIC targeting of the *IGF1R* pathway affected the formation of tumor spheres. After *IGF1R* knockdown, MDA-MB-231 cells exhibited a significant reduction in tumor spheres as compared with CTL control cells (Figures 3B and 3C).

We then tested the activity of ALIC targeting in altering cell migration and invasion. Using the Transwell assay, we showed that ALIC targeting significantly decreased cell migration in both cell clones (Figures 3D and 3E). For cell invasion, MDA-MB-231 cells were seeded on a Matrigel-coated Transwell chamber after the ALIC knockdown of

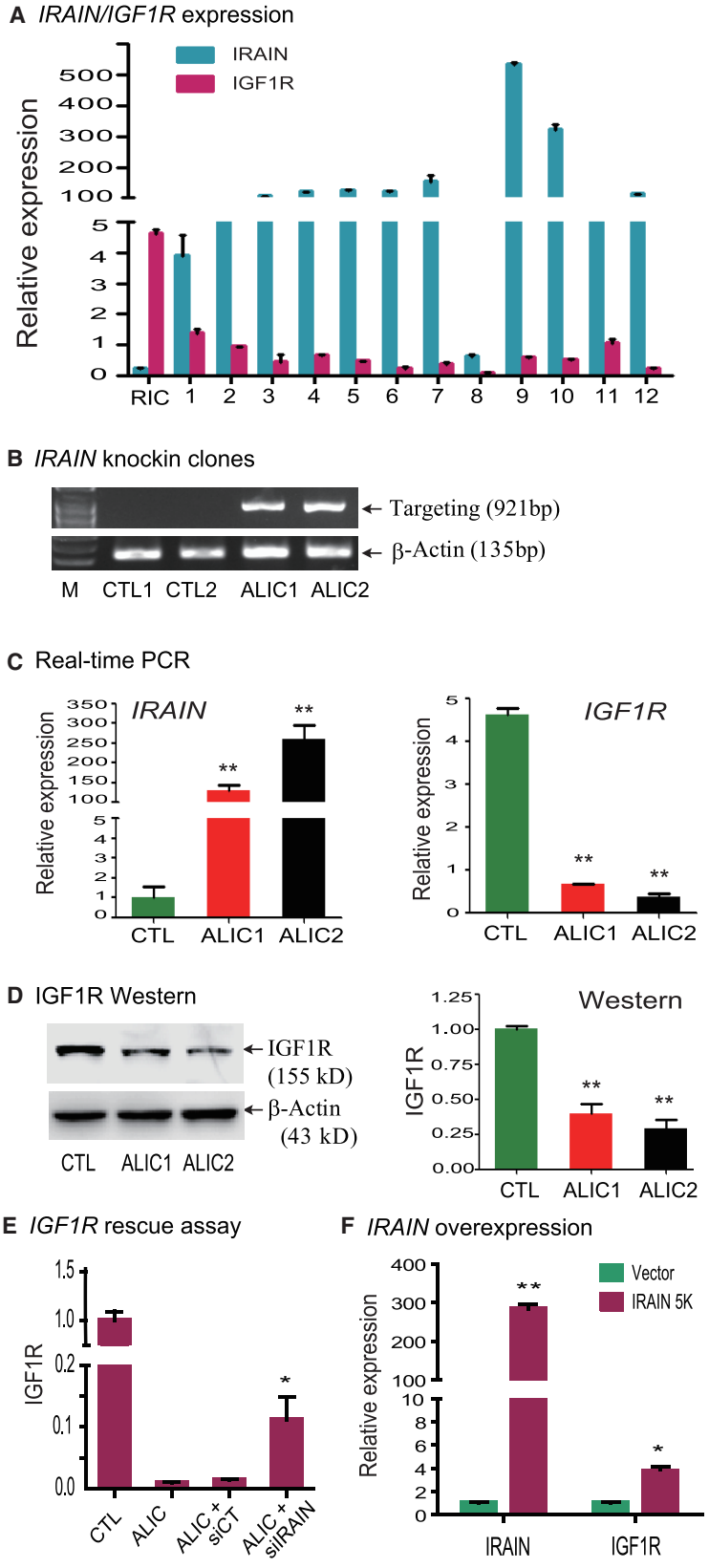

Figure 2. Downregulation of *IGF1R* by *cis* Competition of the Active *IRAIN* Antisense RNA

(A) Reciprocal transcription competition between the sense *IGF1R* mRNA and the antisense *IRAIN* lncRNA. RIC, random insertion control cells. Clones 1–12, cells that carry the *IGF1R* targeting allele in the genome. The abundance of *IGF1R*/*IRAIN* transcripts was measured by qPCR. The data shown are mean ± SD of three independent PCR reactions. Note the downregulated *IGF1R* in clone cells. (B) ALIC targeting of *IGF1R* in two selected cell clones. ALIC1 and ALIC2, ALIC-targeted cells that were transfected with Cre-Neo vector DNA and selected by G418 to remove the puromycin selection marker in the genome. CTL, control cells that carry the random insertion of donor vector were transfected with Cre-Neo vector DNA and selected by G418. ALIC1-2 clone cells carry the targeting allele. (C) Downregulation of *IGF1R* by *cis* competition in two selected cell clones (ALIC1 and ALIC2). Real-time PCR was performed to quantitate the expression level of *IGF1R* and *IRAIN*. All data shown are mean ± SD. $^{**}p < 0.01$ as compared with the control cells (CTL). (D) Western blot of *IGF1R* in targeted cell clones. $^{**}p < 0.01$ as compared with the control cells (CTL). All data shown are mean ± SD. (E) *IGF1R* rescue assay. The CMV promoter-*IRAIN* knockin (ALIC) cells were treated with *IRAIN* siRNA (siIRAIN) and control siRNA (siCT) using lipofectamine RNAiMax. Forty-eight hours after transfection, cells were collected for the measurement of *IGF1R* using qPCR. The PCR value was standardized by setting the CTL control as 1. Error bars represent the SE of the average of three independent PCR reactions. All data shown are mean ± SD. $^{*}p < 0.05$ as compared with the siCT control. (F) *IRAIN* overexpression assay. MDA-MB-231 tumor cells were infected with lentiviruses carrying the 5K *IRAIN* cDNA insert or the copGFP vector control. After viral infection, cells were selected by puromycin and were collected for the quantitation of *IRAIN* and *IGF1R* using qPCR. The copGFP vector control was set as 1 for standardization. Error bars represent the SE of the average of three independent PCR reactions. All data shown are mean ± SD. $^{**}p < 0.01$, $^{*}p < 0.05$ as compared with the vector control.

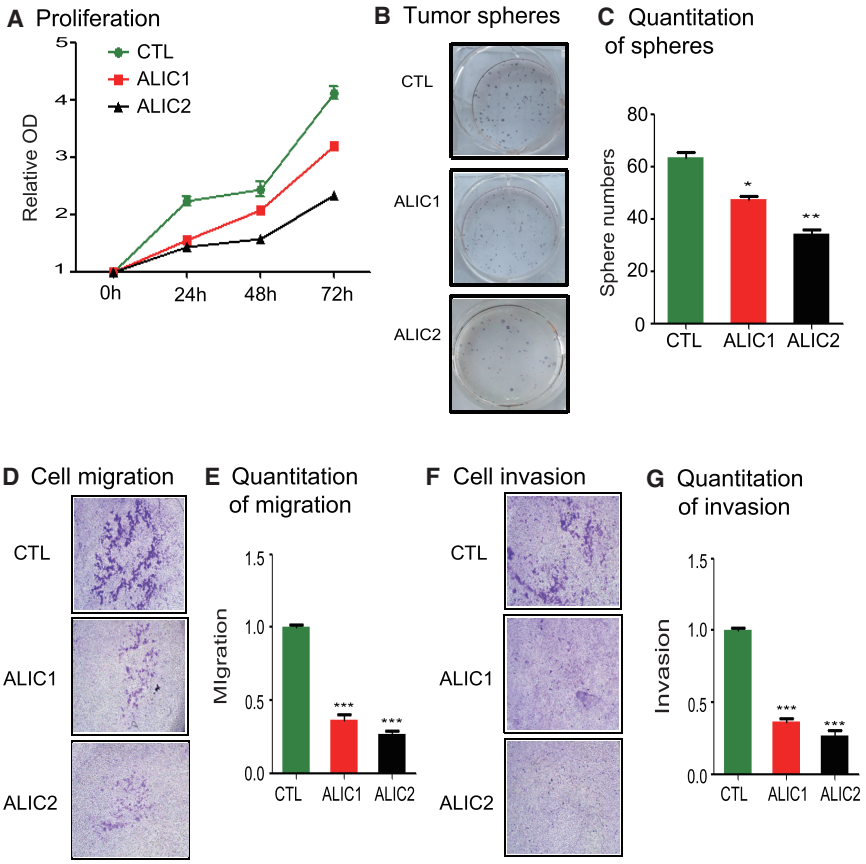

Figure 3. Correction of the Abnormal *IGF1R/IRAIN* Production Alters the Phenotypes of Tumor Cells

(A) Cell proliferation. After ALIC targeting, two cell clones were collected for analysis of cell proliferation using the MTT assay. Cell growth was measured as the relative absorbance by setting 0 hour as 1. All experiments were performed in triplicate. The data shown are mean ± SD. (B) Tumor sphere colonies as measured by the soft agar assay. MDA-MB-231 cell colonies were stained on day 15. (C) Quantitation of tumor sphere colonies. Tumor spheres were stained by 0.005% crystal violet and quantitated as the average sphere colonies per microscope field. All data shown are mean ± SD. *$p < 0.05$, **$p < 0.01$ as compared with the CTL control. (D) Migration of MBA231 cells. Cell migration was measured by insert plate assay. (E) Quantitation of migrated cells. Cell growth was measured as absorbance at 590 nm. All data shown are mean ± SD. ***$p < 0.001$ as compared with the CTL control. Note the decreased cell migration in the two targeted cell clones. (F) Cell invasion. Cells that invaded through the collagen-coated membrane of the Transwell were stained with crystal violet 24 hr after cell seeding. (G) Quantitation of invaded cells. Cell growth was measured as absorbance at 590 nm. All data shown are mean ± SD. ***$p < 0.001$ as compared with the CTL control.

IGF1R. The number of cells that passed through the Matrigel to the bottom of the insert was quantified. The CTL control cells exhibited the malignant phenotype of invading across the Matrigel membrane. However, ALIC targeting of *IGF1R* resulted in significantly decreased invasion activity (Figures 3F and 3G; $p < 0.01$).

Downregulation of the IGF1R Pathway Results in S Phase Cell Cycle Arrest

We used flow cytometry to analyze cell cycle in ALIC-targeting clone cells (Figure 4). After *IGF1R* knockdown by ALIC targeting, there was an increase in the number of cells in S phase (23.3% in CTL cells versus 32.20% in clone #1 and 40.1% in clone #2). In parallel, there was a decrease in the number of cells in G2 phase in the targeted breast cancer cells.

CpG Methylation in the IGF1R Promoter

We examined if the ALIC targeting altered the epigenotype in the overlapping *IGF1R* promoter. Sodium bisulfite sequencing was used to compare the status of DNA methylation in the *IGF1R* promoter (Figure 5A).

In CTL control cells that were transfected with the Cre-Neo control vector in parallel with the ALIC cells, there was minimal DNA methylation of CpG islands at region #1 near the proximal promoter region. In two targeted cell clones, we did not detect any changes in DNA methylation at the CpG sites (Figure 5B). Similarly, there were no changes in the level of CpG methylation in the distal promoter region (Figure 5C). Thus, the antisense tumor suppressor lncRNA-induced suppression of *IGF1R* is not associated with the epigenetic modification in the promoter region.[20]

Identification of Genome-wide Targets of IRAIN lncRNA

To examine if *IRAIN* might also target other genes, we used a "nuclear lncRNA reverse transcription-associated trap" (RAT) method[20,24] to identify a gene network associated with *IRAIN* lncRNA (Figure S4). After crosslinking the chromatin, *IRAIN* lncRNA was first reverse transcribed *in situ* in the nucleus using *IRAIN*-specific complementary primers (Table S1) in a reaction mixture containing biotin-deoxycytidine triphosphate (dCTP). The *IRAIN*-interacting chromatin complex was pulled down with streptavidin beads, and target gene DNAs were purified for library construction and DNA sequencing. By RAT-Seq, we found that in addition to *IGF1R*, *IRAIN* lncRNA also bound to many gene targets that are closely related to tumor progression (Figure 6A). The Kyoto Encyclopedia of Genes and Genomes (KEGG) pathway analysis revealed that *IRAIN* lncRNA might be involved in many signal pathways that are related to tumor growth (Figures 6B and S5). *IRAIN* binds to its gene targets with consensus motif sequences containing poly(A)s and poly(G)s (Figure 6C).

We then used qPCR to measure the mRNA abundance of several *IRAIN* target genes (Figure 6D) in ALIC-targeted cells, including *NM23*, *RHOG*, *PID1*, *IGF2R*, and *FKBP2*. Although the ALIC

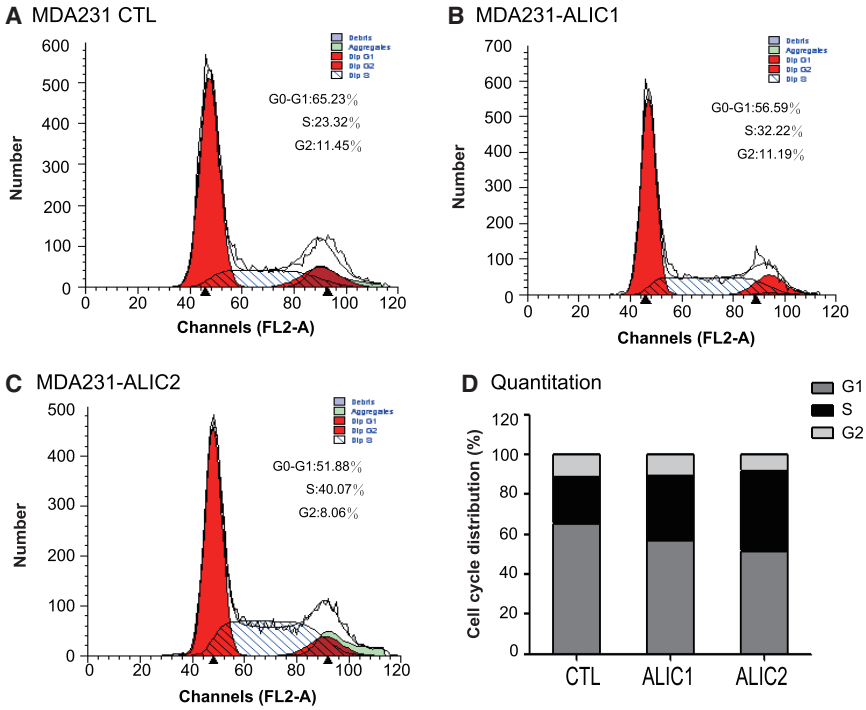

Figure 4. Cell Cycle Analysis

(A–C) FACS analysis of MDA-MB-231 cells after the *IGF1R cis* competition targeting by upregulating *IRAIN*. ALIC1 (B), ALIC2 (C), targeting clones; CTL (A), control cells. (D) Quantitation of the cell cycle.

targeting did not significantly affect all target genes examined, *NM23* and *FKBP3* were dramatically upregulated in ALIC cells. Similarly, the lentivirus-overexpressed *IRAIN* also affected these target genes in MDA-MB-231 breast cancer cells (Figure S6). *NM23* is a well-established metastasis suppressor.[25,26] Thus, *IRAIN* may affect tumor cell growth by regulating its downstream gene targets.

DISCUSSION

The increased activation of the *IGF1R* pathway is a well-established target for breast cancer drug therapy. We have recently identified *IRAIN*, an intragenic antisense lncRNA in the *IGF1R* locus. *IRAIN* is s tumor suppressor that may function as a "*cis* regulatory competitor" to compete with the overlapping promoter of *IGF1R*.[20] In breast cancer, *IRAIN* lncRNA is downregulated.[21] Lack of antisense *cis* competition releases the suppression of the *IGF1R* promoter. The activated *IGF1R* is associated with breast cancer metastasis. We have developed an ALIC strategy to correct the aberrant *IGF1R*/*IRAIN* pathway. In this approach, the weak promoter of *IRAIN* in tumors is activated by CRISPR Cas9 gene editing. The increased transcription of *IRAIN* competes in *cis* with the overlapping *IGF1R* promoter, leading to a rebalance of *IGF1R*/*IRAIN* transcription. Thus, this study may present a useful strategy to precisely target the aberrantly upregulated *IGF1R* pathway in breast cancer cells.

CRISPR-Cas9 technology has been employed as a simple, efficient, and relatively inexpensive technology to precisely edit genes for various applications, including transcriptional regulation, epigenetic control, and chromosome translocation.[27–29] Recently, this editing system has been harnessed to correct disease genes in human embryo genomes.[30–32] By tethering the C terminus of the catalytically inactive dCas9 to three epigenetic suppressor domains, we found that the synthetic dCas9 epi-suppressor gRNAs induced significant decreases in the transcription activity of the *GRN* target gene promoter in Hep3B hepatoma cells.[33] In this study, we have successfully applied the Cas9 system to introduce a powerful promoter in front of the *IRAIN* lncRNA. The Cas9-mediated ALIC approach leads to an increase in *IRAIN* antisense lncRNA, which induces the downregulation of the sense *IGF1R* coding RNA through the *cis* transcription competition over the overlapping promoter.

It is known that several lncRNAs regulate their target genes in *cis* by directly binding to their promoters and enhancers.[34–36] *Airn* is expressed on mouse chromosome 17 from a paternal promoter located in intron 2 of the *Igf2r* gene, which is expressed exclusively from the maternal allele. *Airn* transcriptionally overlaps the *Igf2r* promoter. *Airn* expression is necessary to initiate the *cis* paternal-specific silencing of the *Igf2r* gene.[37,38] In developing ventral forebrain, *Evf2* lncRNA controls expression of Dlx5, Dlx6, and Gad1 in both *trans* and *cis* by recruiting DLX and MECP2 transcription factors to important DNA regulatory elements in the intergenic region.[39] Expression of lncRNAs is required for initiating X chromosome inactivation.[40–43] For example, the spreading of *Xist* lncRNA along one X chromosome in *cis* initiates chromosome-wide silencing. The *X (inactive)-specific transcript, antisense* (*Tsix*) overlaps with the entire *Xist* gene in an antisense orientation and silences *Xist* on the active X chromosome. Previously, we demonstrated that *Kcnq1ot1* lncRNA uses its 5′ region RNA as a scaffold to orchestrate a long-range intrachromosomal loop between the imprinting control region $KvDMR_1$ and the *Kcnq1* promoter. With this spatial proximity, the imprinting signal in the $KvDMR_1$ can be directly delivered to the *Kcnq1* promoter in *cis*.[44] Additionally, many enhancer DNA elements can encode unpolyadenylated enhancer RNAs (eRNAs) that tightly regulate neighboring coding genes.[45,46] However, these eRNAs function primarily as activators rather than repressors when targeting promoters.[47,48]

In the current study, using the CRISPRCas9 gene-editing system, we also show that the actively transcribed *IRAIN* antisense lncRNA is able to downregulate in *cis* the expression of the overlapping *IGF1R*. These data suggest a useful approach to modulate gene activity efficiently using a *cis* competition mechanism. This is in contrast to

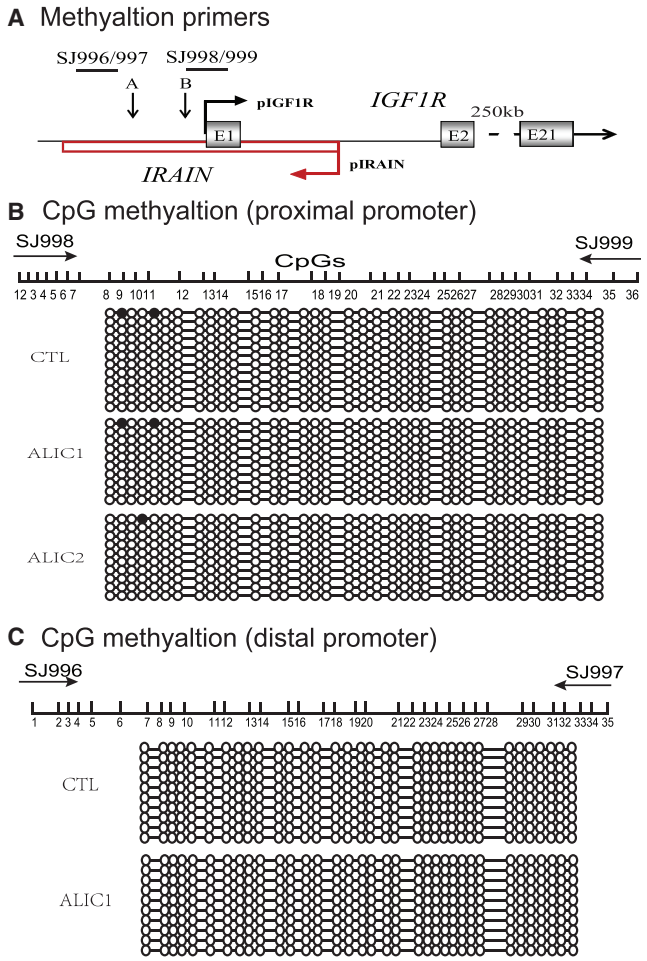

Figure 5. The Status of DNA Methylation in the *IGF1R* Promoters

(A) Schematic diagram of the *IGF1R/IRAIN* gene locus and the location of PCR primers. (B) CpG DNA methylation of site 1. Genomic DNAs were extracted from breast cancer cells. After treated with sodium sulfite, the *IRAIN* promoter DNA was amplified and sequenced. Open circles, unmethylated CpGs; solid circles, methylated CpGs. All the CpG islands were unmethylated in both the CTL control and ALIC-targeted cells. (C) CpG DNA methylation of site 2. Note the equal DNA hypomethylation in both the CTL control and ALIC-targeted cells.

siRNA and locked nucleic acids (LNA) oligo techniques, which function at the posttranscriptional level. siRNAs bind to the target RNA and induce RNA degradation by the Dicer-Ago2 pathway, inducing the inhibition of gene expression or translation. The data from our rescue assay also demonstrate that the *IRAIN* siRNA rescue experiment only shows a minor restoration in *IGF1R* mRNA levels, while *IRAIN* levels are almost back to normal levels. The siRNA-mediated post-transcriptional knockdown of *IRAIN* cannot fully counteract the *cis* inhibition of *IGF1R* induced by ALIC targeting. This suggests that it is not the sequence of IRAIN but the *cis* transcription competition that is most important of the effect on *IGF1R*. Future studies are needed to address whether the siRNA-mediated knockdown in the rescue assay or the *trans* overexpressed *IRAIN* is able to alter the phenotypes in breast cancer cells, including xenograft tumor studies *in vivo*.

Using nuclear RNA RAT sequencing (RAT-Seq), we have identified a gene network associated with *IRAIN* lncRNA. We found that *IRAIN* bound to many target genes that are closely related to tumor progression. We used qPCR to quantitate target genes in ALIC-targeted cells, including *NM23*, *RHOG*, *PID1*, *IGF2R*, and *FKBP3*. Among them, *NM23* and *FKBP3* were significantly upregulated in ALIC cells. *NM23* has been extensively studied for its role as a metastasis suppressor.[25,26] In humans, at least eight *NM23* family genes that encode for nucleoside diphosphate kinases or for homologous isoforms have been identified. *NM23* participates in the regulation of a broad spectrum of cellular pathways involved in development, differentiation, proliferation, endocytosis, and apoptosis.[49,50] Ectopic expression of *NM23* has been shown to reduce metastasis in several tumor models.[51] The molecular mechanisms for the role of *NM23* as a metastasis suppressor have so far remained unclear. There is a suggestion that NM23 and its interacting partner STRAP may physically interact with p53 and positively regulate p53-induced apoptosis and cell cycle arrest.[52] In addition, *NM23* may regulate many genes with relevance to breast cancer, including *MET*, *EDG2*, *L1CAM*, *SMO*, and *PTN*.[53] *FKBP3* (FK506-binding protein 3), a member of the immunophilin protein family, plays a role in immunoregulation and basic cellular processes involving protein folding and trafficking by binding to the immunosuppressants FK506 and rapamycin.[54] We found that ectopic expression of the *IRAIN* 5K cDNA also significantly upregulated *FKBP3* (Figure S6). Thus, *IRAIN* may also directly affect tumor metastasis by affecting its downstream gene targets, like *NM23* metastasis suppressor.

In summary, the *IGF1R-IRAIN* locus is dysregulated in breast cancers due to the upregulated *IGF1R* growth signal and the downregulated *IRAIN* lncRNA tumor suppressor. We show that targeted activation of *IRAIN* by ALIC targeting suppressed *IGF1R* using a *cis* competition mechanism. Rebalance of the *IGF1R* pathway provides a molecular basis for the development of precision therapy against breast cancer. Thus, ALIC targeting may provide a useful strategy to target *IGF1R* in precision tumor therapy. Future studies are needed to learn if ALIC can be used to develop novel therapies against other cancer target genes that may not have an antisense lncRNA.

MATERIALS AND METHODS

Construction of the IGF1R Targeting and Donor Vectors

In breast cancer cells, *IGF1R* is upregulated in parallel with the downregulated *IRAIN* tumor suppressor lncRNA. To precisely target this unbalanced *IGF1R/IRAIN* pathway, we used a CRISPRCas9 gene-editing system to activate the weak *IRAIN* promoter in breast cancer cells (Figures 1A and 1B). We constructed the Cas9-*IRAIN*-gRNA-targeting vector by cloning two *IRAIN* promoter gRNAs into the lenti-CRISPR-EGFP-gRNA vector (Addgene Plasmid #51761). A U6-gRNA1-T5-H1-gRNA2 cassette was synthesized by joining the H1 promoter with gRNA oligonucleotides from the *IRAIN* promoter: *IRAIN*-gRNA1, 5′-GCCCCAGTCCGCGTCCCACT-3′; *IRAIN*-gRNA2,

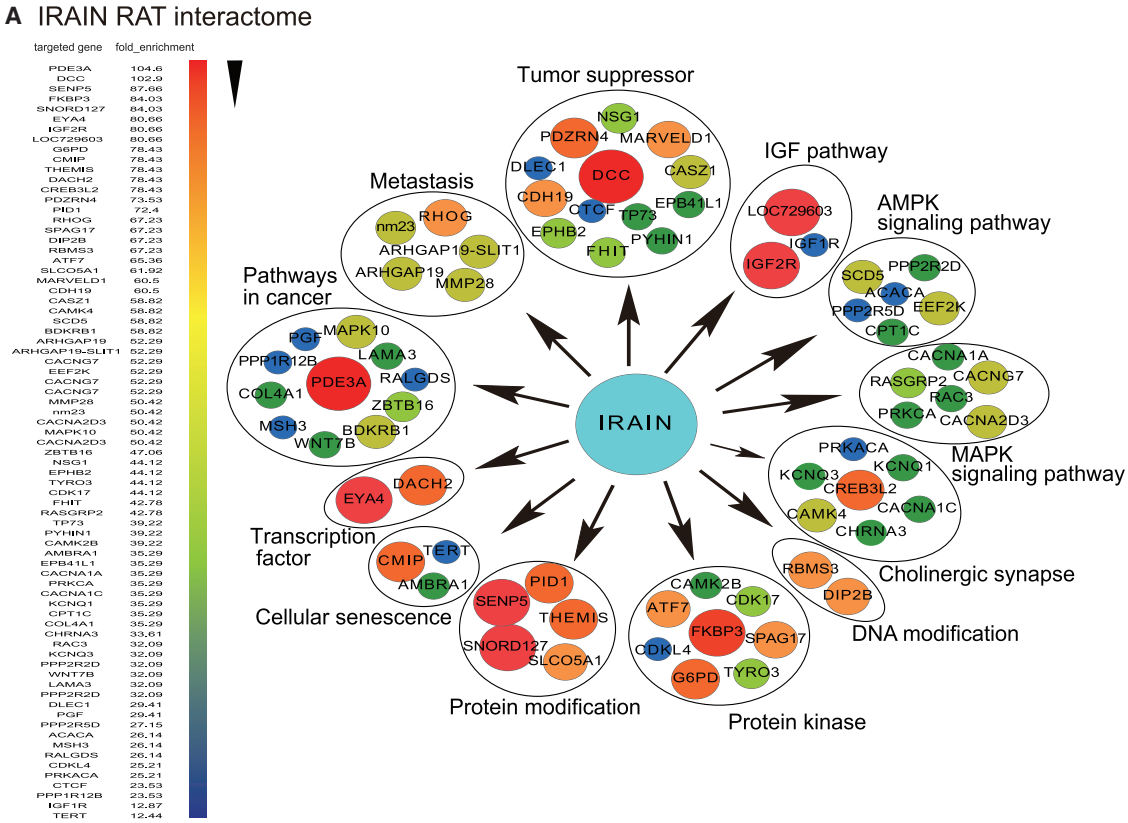

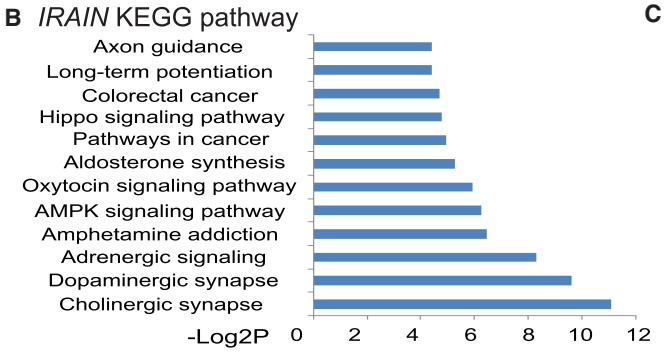

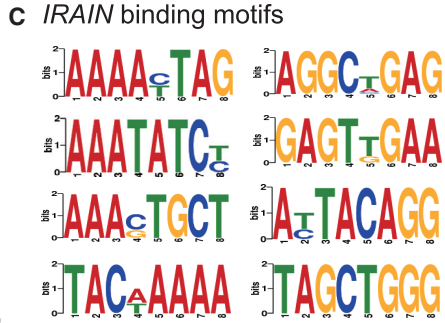

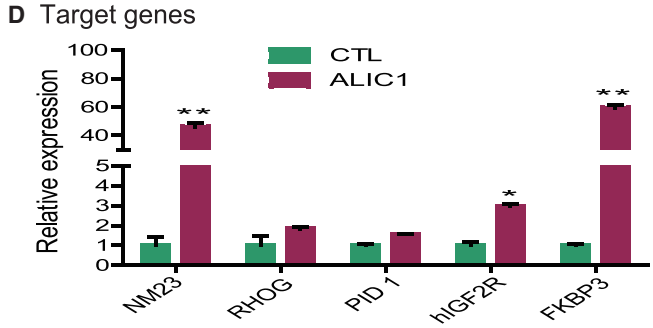

(legend on next page)

5′-CATTTCTTACCAGACGTTTA-3′; *IRAIN*-gRNA3, 5′-CCACCT AAACGACTTAGTAA-3′; *IRAIN*-gRNA4, 5′-GCCCAGATCTGTG GAAGGTC-3′; respectively (Figures S1A and S1B). The expression cassette was inserted downstream of the U6 promoter in the vector using Pme I and Not I.

The donor vector was constructed by PCR amplification of two arm fragments from the *IRAIN* locus and cloned into a targeting vector containing both the pCMV-loxP-puromycin-loxP positive selection cassette and the pPGK-thymidine kinase (TK) negative selection marker (Figure 1C).[55] Two arm fragments were amplified from the human genome DNA using the following primers: SJ016F, 5′-TCAA AATTTTATCGATATTATCTGGCTATCACTCAGAACCT-3′, and SJ017, 5′-GCGTATATCTGGCCCGTACATCTTCGAAGATAAGT ACGGTTTAGAAGACACG-3′ for the Arm 1 fragment; and SJ022, 5′-CTGAGTCGACTCTAGACAGCCTTTCTGAATTGCCCC GGT-3′, and SJ023, 5′-TTAAATCGACGCTAGCCCTCGGCTGT GACCTTCAGCGAGC-3′ for the Arm 2 fragment. They were cloned into the Cas9 donor vector using Cla1/BsrG1 and Xba1/Nhe1 sites, respectively. The pCMV-controlled puromycin in the vector was used as the positive selection marker and the pPGK-TK cassette as the negative selection marker.

Targeting the IGF1R/IRAIN Pathway in Breast Cancer Cells

IGF1R targeting was accomplished by introducing a strong CMV promoter immediately upstream of *IRAIN* using the CRISPRCas9 gene-editing system. First, the *IGF1R* locus was targeted by Cas9 using four *IGF1R* gRNAs in two targeting vectors. Second, a donor vector that contains a strong CMV promoter was used to target the *IGF1R* locus through homologous recommendation. After targeting, the CMV promoter drove the overexpression of the antisense *IRAIN* lncRNA, which in turn competes with the transcription of the sense *IGF1R* coding mRNA (Figure 1C).

Breast cancer cell line MDA-MB-231 was purchased from American Type Culture Collection (ATCC). Cells were grown in RP1640 media, supplemented with 10% fetal bovine serum (FBS), 100 U/mL penicillin, and 100 μg/mL streptomycin. Both the targeting vector and the donor vectors were co-transfected into MDA-MB-231 cells using Lipofectamine 2000 (Invitrogen, CA) following the protocol provided by the kit. Two days after co-transfection, cells were positively selected using 1 mg/mL puromycin for 3 days and then were negatively selected using 250 μM ganciclovir[55] (Figure S1C). Treatment of cells with ganciclovir should reduce the random insertion of the donor vector in the genome. A total of twelve stable cell clones were collected, and genomic DNA was purified to screen for homologous knockin recombination, using primers located in the genomic DNA and vectors (Table S1). As the study control, MDA-MB-231 cells were transfected with only the donor vector DNA and were selected with puromycin. These control cells contained randomly inserted donor vector DNA in the genome (RIC cells).

Removal of Puromycin Selection Marker in Targeting Cells

Among targeted cells, clone 7 cells that contained the minimum randomly integrated vector DNA were selected for the study. The cells were transfected with a pCMV-Cre-Neo vector DNA using Lipofectamine 2000 (Invitrogen, CA) and were treated with G418 (1 mg/mL, Invitrogen, CA). The expression of the Cre recombinase removed the puromycin marker gene at the targeted *IGF1R* and *IRAIN* loci and generated the pCMV-*IRAIN* knockin cells (ALIC targeting). As a control, RIC cells that carry the random insertion of the donor vector DNA were also transfected with pCMV-Cre-Neo DNA and were treated with G418 in parallel with the ALIC cells (CTL cells).

Validation of ALIC Targeting by DNA Sequencing

ALIC targeting produced cell clones that contain some randomly inserted donor vector DNA, which may interfere with the signal in Southern blotting. Thus, we used PCR to amplify the entire targeted region and confirmed ALIC targeting by DNA sequencing. The targeted region was amplified by primers SJ131 and JH583 (Table S1) and was cloned into a pJet vector for sequencing. The regions covering the donor arms and the inserted promoter were validated by DNA sequencing.

Quantitation of IGF1R/IRAIN Expression

Total RNA was extracted from tissues by TRI-REAGENT (Sigma, CA), and cDNA was synthesized with RNA reverse transcriptase as previously described.[56,57] The resulting cDNA was used to quantitate the expression of *IGF1R* coding RNA and *IRAIN* lncRNA using primers listed in Table S1. In brief, PCR was performed under liquid wax in a 6 μL reaction containing 2 μL of 3 × Klen-T*aq*I Mix, 2 μL cDNA, and 1 μL of each 2.5 μM primer. After incubation at 95°C for 2 min, *IGF1R* and *IRAIN* cDNAs were amplified by 32 cycles of 95°C for 30 s, 65°C for 30 s of annealing, and 72°C for 35 s of extension, and finally with extension at 72°C for 5 min. Amplified PCR products of the expected size were quantified by densitometric measurements and normalized to β-actin values. For qPCR analysis, cDNA samples were amplified using CFX96 real-time system (Bio-Rad) by SYBR PrimeScript RT-PCR Kit (Takara). mRNA levels were quantitated by normalizing Ct value over β-actin (housekeeping gene) as previously described.[58]

The IGF1R-Targeting Rescue Assay

To further test the role of ALIC targeting, we determined whether the phenotypes of the *IGF1R*-targeted cells could be rescued by knockdown of *IRAIN* using siRNAs. Three *IRAIN*-specific RNAi

Figure 6. *IRAIN* lncRNA Binding Targets

(A) The *IRAIN* lncRNA interactome. The *IRAIN* RNA interaction was drawn based on the enrichment of the top RAT-Seq pathway target genes. (B) The KEGG pathway of *IRAIN* lncRNA targets. (C) The consensus binding motifs of *IRAIN* lncRNA. (D) Quantitation of *IRAIN* target genes in ALIC1-targeted cells. Gene expression was measured by qPCR. The values were standardized by setting the CTL control as 1. Error bars represent the SE of the average of three independent PCR reactions. All data shown are mean ± SD. *$p < 0.05$, **$p < 0.01$ as compared with the CTL control.

oligonucleotides were chemically synthesized by Wiewsolid Biotech (Beijing, China). Cells were plated in 6-well plates at 5×10^5 per well. Twenty-four hours after plating, 40 pmol of si*IRAIN* and scramble controls siCTs (Table S1) were transfected into cells using Lipofectamine RNAiMax (Invitrogen, CA) following the manufacturer's protocol. Forty-eight hours after transfection, cells were collected and total RNA was isolated using Trizol (Sigma, MO). The expression of *IGF1R* and *IRAIN* was measured by qPCR.

IRAIN Overexpression Assay

To examine whether a virally expressed *IRAIN* lncRNA would affect *IGF1R* in *trans*, we overexpressed *IRAIN* in MDA-MB-231 tumor cells. As previously reported,[20] a 5.4-kb full-length *IRAIN* cDNA was cloned into pCMV-copGFP/Puro vector to construct the *IRAIN* 5K cDNA vector (IRAIN5K). Lentiviruses were packaged in 293 cells and were used to infect MDA-MB-231 cells. As a control, MDA-MB-231 cells were infected with the CMV-copGFP/Puro empty vector (Vector). After puromycin selection, cells that stably expressed *IRAIN* or the control vector were collected for gene analysis. qPCR was used to measure the expression of *IGF1R* and target genes.

Western Blot Analysis of IGF1R in ALIC-Targeted Cells

Total cell protein was extracted with radioimmunoprecipitation assay (RIPA) buffer supplemented with cocktail protease inhibitor (Roche), and the protein concentration was determined by a Pierce BCA protein assay kit as previously described.[59] Twenty micrograms of total cell protein were separated on 12% SDS-PAGE and electrophoretically transferred to polyvinylidene fluoride (PVDF) membranes (0.45 μm, Millipore, Billerica, MA, USA). After blocking with 5% skim milk, the membranes were incubated with monoclonal antibodies against *IGF1R* (Santa Cruz Biotechnology, CA) and were detected with the enhanced chemiluminescence system (ECL, Thermo). Protein expression levels were determined semiquantitatively by densitometric analysis with the Quantity One software (Bio-Rad, CA).[60,61]

RAT Assay

A nuclear lncRNA RAT assay[20,62] was used in this study to determine the genome-wide targets that interact with *IRAIN* lncRNA (Figure S4). In brief, stable MDA-MB-231 clone cells were cross-linked with 2% formaldehyde and lysed with cell lysis buffer (10 mM Tris [pH 8.0], 10 mM NaCl, 0.2% NP-40, 1× protease inhibitors). The nuclei were centrifuged and suspended in 1× reverse transcription buffer, and gene strand-specific reverse transcription was performed *in situ* in the nucleus with biotin-dCTP. The cells were incubated for 50 min with Maxima Reverse Transcriptase (Thermo Fisher Scientific, CA) at 60°C, and the reaction was stopped by heating at 85°C for 5 min. The nuclei were lysed by adding 0.3% SDS at 37°C for 1 hr. Triton X-100 was then added to a final concentration of 1.8% to sequester the SDS. The biotinylated-*IRAIN* cDNA/chromatin DNA complex was purified by streptavidin magic beads (Invitrogen, CA). After washing, the pulled-down sample was treated with 10 mg/mL proteinase K at 65°C overnight to reverse the cross-links. Following incubation with 0.4 μg/mL RNase A for 30 min at 37°C, the *IRAIN* cDNA/DNA was extracted and sonicated on ice using a Branson sonicator. The sonicated DNAs were further digested by *Mbo1* into small fragments and ligated with the NEBNext adaptors (NEBNext ChIP-Seq Library Prep Master Mix Set for Illumina) to construct the library. The library DNAs were subjected to Illumina sequencing by Shanghai Biotechnology (Shanghai, China).

RAT-Seq Data Analysis

The RAT-Seq reads were mapped to the human genome (hg38) using Bowtie2.[63] MACs2 was used to identify the DNA regions that interacted with the *IRAIN* lncRNA. Target genes were obtained from GENCODE[64] and the upstream 2 kb and downstream 1 kb of the transcription start sites were defined as the gene promoter regions. The peaks were visualized using the Integrative Genomics Viewer (IGV) tools.[65,66]

Functional Enrichment Analysis and GSEA

The GseaPreranked tool in GSEAv2.0[67] was used to perform gene set enrichment analysis (GSEA) on gene promoters that were bound by *IRAIN*. We obtained the gene sets from the Gene Set Knowledgebase (GSKB) (https://bioconductor.org/packages/release/data/experiment/html/gskb.html) for pathways and functional categories. The genes that interacted with *IRAIN* were sorted by the qValue (−log10) of the peak signal. Statistical significance was assessed by comparing the enrichment score to enrichment results generated from 1,000 random permutations of the gene sets to obtain p values.

Tumor Sphere-Forming Assay

The tumor clonogenic assay was performed using the method as previously described.[56,68] Cells were digested, centrifuged, and re-suspended in DMEM to form single-cell suspensions. Cells were diluted to 2×10^3 cells/mL in 0.25 mL DMEM-agarose. The plates were incubated at 37°C, 5% CO_2. After ~2 weeks, colonies were visualized by staining with 5 mg/mL 3-(4,5-dimethylthiazol-2-yl)-2,5-diphenyltetrazolium bromide (MTT; Sigma, MO) for 3 hr. Cloning forming efficiency (CFE) was defined as the number of colonies/number of inoculated cells × 100%.

Cell Proliferation Assay

Cell survival was measured using the MTT assay as previously described.[58,69] In brief, cells (1×10^4/well) were plated onto 96-well plates and were incubated with 20 μL 5 mg/mL MTT (Sigma, MO) per well at 37°C for 4 hr. The absorbance was measured at 490 nm. Cell viability (%) was calculated based on the following equation: Cell viability (%)$1/4(A_{sample}/A_{control}) \times 100\%$, where A_{sample} and $A_{control}$ represent the absorbance of the sample and control wells, respectively.

Cell Migration and Invasion Assay

Cell migration and invasion assays were carried out using Transwell membrane filters inserted in 24-well tissue culture plates (6.5-mm diameter, 8-μm pore size) (Corning, MA) following the method as previously described.[70,71] For the migration assay, 4×10^4 cells suspended in serum-free medium were seeded on the top chamber of

Transwell filters. Serum-containing medium was added to the bottom chamber and incubated for 16 hr at 37°C. The nonmigrating cells were removed by wiping the upper side of the filter, and the migrating cells on the bottom side of the filter were fixed with 4% formaldehyde and stained with crystal violet.

Cell invasion was measured using a similar protocol except that cells were seeded in Transwell chambers coated with Matrigel (Invitrogen, CA, USA). Each assay represents the average of three independent experiment.[56]

Cell Cycle Analysis by Flow Cytometry

Cells were washed twice with PBS, pelleted, and fixed with cold 70% ethyl alcohol for at least 30 min. After being washed twice with cold PBS, cells were incubated with 200 μg/mL RNase A for 30 min at 37°C. The cells were stained with 100 μg/mL propidium iodide for 30 min at room temperature. The samples were immediately analyzed by flow cytometry. Cell cycle phase distribution was determined using Cell Quest Pro software.[56,59]

Statistical Analysis

The experimental data are expressed as mean ± SD. Data were analyzed using SPSS software (version 16.0; SPSS, IL). Student's t test or one-way ANOVA (Bonferroni test) was used to compare statistical differences for variables among treatment groups. Results were considered statistically significant at $p < 0.05$.

SUPPLEMENTAL INFORMATION

Supplemental Information includes six figures and one table and can be found with this article online at https://doi.org/10.1016/j.omtn.2018.04.013.

AUTHOR CONTRIBUTIONS

J.-F.H., J.C., J.S., W.L., and S.Z. conceived and designed the study; L.P., X.W., L.K., Z.L., Y.N., Z.D., D.Y., L.Z., L.J., N.C., and D.L. performed the experiments; J.-F.H. wrote the paper; A.R.H. reviewed and edited the manuscript. All authors read and approved the manuscript.

CONFLICTS OF INTEREST

No potential conflicts of interest were disclosed.

ACKNOWLEDGMENTS

This work was supported by the National Natural Science Foundation of China (grants 31430021 and 81272294), the National Basic Research Program of China (973 Program) (2015CB943303), the Natural Science Foundation of Jilin Science and Technique (grant 20180101117JC), and the California Institute of Regenerative Medicine (CIRM) (grant RT2-01942) to J.-F.H.; the National Natural Science Foundation of China (grants 81372835 and 81670143) and the Jilin Science and Technique International Collaboration (grant 20130413010GH) to W.L.; the Key Project of Chinese Ministry of Education (grant 311015), the National Natural Science Foundation of China (grant 81672275), the National Key Research and Development Program of China (grant 2016YFC13038000), the Natural Science Foundation of Jilin Province (grant 20150101176JC), the Research on Chronic Noncommunicable Diseases Prevention and Control of National Ministry of Science and Technology (grant 2016YFC1303804), and the National Health Development Planning Commission Major Disease Prevention and Control of Science and Technology Plan of Action, Cancer Prevention and Control (grant ZX-07-C2016004) to J.C.; the Junior National Natural Science Foundation of China (grant #81502277) to L.K.; the Junior National Natural Science Foundation of China (grant #81600150) and the Bethune B project grant of Jilin University (#2015211) to J.S.; the Jilin Science and Technique International Collaboration grant (20180414065GH) to D.Y.; and the Department of Veterans Affairs.

REFERENCES

1. Devin, J.L., Bolam, K.A., Jenkins, D.G., and Skinner, T.L. (2016). The influence of exercise on the insulin-like growth factor axis in oncology: physiological basis, current, and future perspectives. Cancer Epidemiol. Biomarkers Prev. *25*, 239–249.

2. Singh, P., Alex, J.M., and Bast, F. (2014). Insulin receptor (IR) and insulin-like growth factor receptor 1 (IGF-1R) signaling systems: novel treatment strategies for cancer. Med. Oncol. *31*, 805.

3. Kasprzak, A., Kwasniewski, W., Adamek, A., and Gozdzicka-Jozefiak, A. (2017). Insulin-like growth factor (IGF) axis in cancerogenesis. Mutat. Res. Rev. Mutat. Res. *772*, 78–104.

4. Solarek, W., Czarnecka, A.M., Escudier, B., Bielecka, Z.F., Lian, F., and Szczylik, C. (2015). Insulin and IGFs in renal cancer risk and progression. Endocr. Relat. Cancer *22*, R253–R264.

5. Denduluri, S.K., Idowu, O., Wang, Z., Liao, Z., Yan, Z., Mohammed, M.K., Ye, J., Wei, Q., Wang, J., Zhao, L., and Luu, H.H. (2015). Insulin-like growth factor (IGF) signaling in tumorigenesis and the development of cancer drug resistance. Genes Dis. *2*, 13–25.

6. Motallebnezhad, M., Aghebati-Maleki, L., Jadidi-Niaragh, F., Nickho, H., Samadi-Kafil, H., Shamsasenjan, K., and Yousefi, M. (2016). The insulin-like growth factor-I receptor (IGF-IR) in breast cancer: biology and treatment strategies. Tumour Biol. *37*, 11711–11721.

7. Bergman, D., Halje, M., Nordin, M., and Engström, W. (2013). Insulin-like growth factor 2 in development and disease: a mini-review. Gerontology *59*, 240–249.

8. Voudouri, K., Berdiaki, A., Tzardi, M., Tzanakakis, G.N., and Nikitovic, D. (2015). Insulin-like growth factor and epidermal growth factor signaling in breast cancer cell growth: focus on endocrine resistant disease. Anal. Cell. Pathol. (Amst.) *2015*, 975495.

9. Chapuis, N., Tamburini, J., Cornillet-Lefebvre, P., Gillot, L., Bardet, V., Willems, L., Park, S., Green, A.S., Ifrah, N., Dreyfus, F., et al. (2010). Autocrine IGF-1/IGF-1R signaling is responsible for constitutive PI3K/Akt activation in acute myeloid leukemia: therapeutic value of neutralizing anti-IGF-1R antibody. Haematologica *95*, 415–423.

10. Gallardo, A., Lerma, E., Escuin, D., Tibau, A., Muñoz, J., Ojeda, B., Barnadas, A., Adrover, E., Sánchez-Tejada, L., Giner, D., et al. (2012). Increased signalling of EGFR and IGF1R, and deregulation of PTEN/PI3K/Akt pathway are related with trastuzumab resistance in HER2 breast carcinomas. Br. J. Cancer *106*, 1367–1373.

11. Pollak, M. (2012). The insulin and insulin-like growth factor receptor family in neoplasia: an update. Nat. Rev. Cancer *12*, 159–169.

12. Pierre-Eugene, C., Pagesy, P., Nguyen, T.T., Neuillé, M., Tschank, G., Tennagels, N., Hampe, C., and Issad, T. (2012). Effect of insulin analogues on insulin/IGF1 hybrid receptors: increased activation by glargine but not by its metabolites M1 and M2. PLoS ONE *7*, e41992.

13. Danielsen, S.A., Eide, P.W., Nesbakken, A., Guren, T., Leithe, E., and Lothe, R.A. (2015). Portrait of the PI3K/AKT pathway in colorectal cancer. Biochim. Biophys. Acta *1855*, 104–121.

14. Farabaugh, S.M., Boone, D.N., and Lee, A.V. (2015). Role of IGF1R in breast cancer subtypes, stemness, and lineage differentiation. Front. Endocrinol. (Lausanne) *6*, 59.

15. Rieder, S., Michalski, C.W., Friess, H., and Kleeff, J. (2011). Insulin-like growth factor signaling as a therapeutic target in pancreatic cancer. Anticancer. Agents Med. Chem. *11*, 427–433.

16. Marzec, K.A., Baxter, R.C., and Martin, J.L. (2015). Targeting insulin-like growth factor binding protein-3 signaling in triple-negative breast cancer. BioMed Res. Int. *2015*, 638526.

17. Ochnik, A.M., and Baxter, R.C. (2016). Combination therapy approaches to target insulin-like growth factor receptor signaling in breast cancer. Endocr. Relat. Cancer *23*, R513–R536.

18. Chen, H.X., and Sharon, E. (2013). IGF-1R as an anti-cancer target—trials and tribulations. Chin. J. Cancer *32*, 242–252.

19. Beckwith, H., and Yee, D. (2015). Minireview: were the IGF signaling inhibitors all bad? Mol. Endocrinol. *29*, 1549–1557.

20. Sun, J., Li, W., Sun, Y., Yu, D., Wen, X., Wang, H., Cui, J., Wang, G., Hoffman, A.R., and Hu, J.F. (2014). A novel antisense long noncoding RNA within the IGF1R gene locus is imprinted in hematopoietic malignancies. Nucleic Acids Res. *42*, 9588–9601.

21. Kang, L., Sun, J., Wen, X., Cui, J., Wang, G., Hoffman, A.R., Hu, J.F., and Li, W. (2015). Aberrant allele-switch imprinting of a novel IGF1R intragenic antisense non-coding RNA in breast cancers. Eur. J. Cancer *51*, 260–270.

22. Feng, J., Sun, Y., Zhang, E.B., Lu, X.Y., Jin, S.D., and Guo, R.H. (2015). A novel long noncoding RNA IRAIN regulates cell proliferation in non small cell lung cancer. Int. J. Clin. Exp. Pathol. *8*, 12268–12275.

23. Lian, Y., Wang, J., Feng, J., Ding, J., Ma, Z., Li, J., Peng, P., De, W., and Wang, K. (2016). Long non-coding RNA IRAIN suppresses apoptosis and promotes proliferation by binding to LSD1 and EZH2 in pancreatic cancer. Tumour Biol. *37*, 14929–14937.

24. Wang, H., Ge, S., Qian, G., Li, W., Cui, J., Wang, G., Hoffman, A.R., and Hu, J.F. (2015). Restoration of IGF2 imprinting by polycomb repressive complex 2 docking factor SUZ12 in colon cancer cells. Exp. Cell Res. *338*, 214–221.

25. Takács-Vellai, K. (2014). The metastasis suppressor Nm23 as a modulator of Ras/ERK signaling. J. Mol. Signal. *9*, 4.

26. Marshall, J.C., Collins, J., Marino, N., and Steeg, P. (2010). The Nm23-H1 metastasis suppressor as a translational target. Eur. J. Cancer *46*, 1278–1282.

27. Donohoue, P.D., Barrangou, R., and May, A.P. (2018). Advances in industrial biotechnology using CRISPR-Cas systems. Trends Biotechnol. *36*, 134–146.

28. Birling, M.C., Herault, Y., and Pavlovic, G. (2017). Modeling human disease in rodents by CRISPR/Cas9 genome editing. Mamm. Genome *28*, 291–301.

29. Higashijima, Y., Hirano, S., Nangaku, M., and Nureki, O. (2017). Applications of the CRISPR-Cas9 system in kidney research. Kidney Int. *92*, 324–335.

30. Liang, P., Xu, Y., Zhang, X., Ding, C., Huang, R., Zhang, Z., Lv, J., Xie, X., Chen, Y., Li, Y., et al. (2015). CRISPR/Cas9-mediated gene editing in human tripronuclear zygotes. Protein Cell *6*, 363–372.

31. Kang, X., He, W., Huang, Y., Yu, Q., Chen, Y., Gao, X., Sun, X., and Fan, Y. (2016). Introducing precise genetic modifications into human 3PN embryos by CRISPR/Cas-mediated genome editing. J. Assist. Reprod. Genet. *33*, 581–588.

32. Tang, L., Zeng, Y., Du, H., Gong, M., Peng, J., Zhang, B., Lei, M., Zhao, F., Wang, W., Li, X., and Liu, J. (2017). CRISPR/Cas9-mediated gene editing in human zygotes using Cas9 protein. Mol. Genet. Genomics *292*, 525–533.

33. Wang, H., Guo, R., Du, Z., Bai, L., Li, L., Cui, J., Li, W., Hoffman, A.R., and Hu, J.-F. (2018). Epigenetic targeting of Granulin in hepatoma cells by synthetic CRISPR dCas9 epi-suppressors. Mol. Ther. Nucleic Acids *11*, 23–33.

34. Engreitz, J.M., Ollikainen, N., and Guttman, M. (2016). Long non-coding RNAs: spatial amplifiers that control nuclear structure and gene expression. Nat. Rev. Mol. Cell Biol. *17*, 756–770.

35. Krishnan, J., and Mishra, R.K. (2014). Emerging trends of long non-coding RNAs in gene activation. FEBS J. *281*, 34–45.

36. Kornienko, A.E., Guenzl, P.M., Barlow, D.P., and Pauler, F.M. (2013). Gene regulation by the act of long non-coding RNA transcription. BMC Biol. *11*, 59.

37. Santoro, F., Mayer, D., Klement, R.M., Warczok, K.E., Stukalov, A., Barlow, D.P., and Pauler, F.M. (2013). Imprinted Igf2r silencing depends on continuous Airn lncRNA expression and is not restricted to a developmental window. Development *140*, 1184–1195.

38. Latos, P.A., Pauler, F.M., Koerner, M.V., Şenergin, H.B., Hudson, Q.J., Stocsits, R.R., Allhoff, W., Stricker, S.H., Klement, R.M., Warczok, K.E., et al. (2012). Airn transcriptional overlap, but not its lncRNA products, induces imprinted Igf2r silencing. Science *338*, 1469–1472.

39. Bond, A.M., Vangompel, M.J., Sametsky, E.A., Clark, M.F., Savage, J.C., Disterhoft, J.F., and Kohtz, J.D. (2009). Balanced gene regulation by an embryonic brain ncRNA is critical for adult hippocampal GABA circuitry. Nat. Neurosci. *12*, 1020–1027.

40. Froberg, J.E., Yang, L., and Lee, J.T. (2013). Guided by RNAs: X-inactivation as a model for lncRNA function. J. Mol. Biol. *425*, 3698–3706.

41. Lee, J.T., and Bartolomei, M.S. (2013). X-inactivation, imprinting, and long noncoding RNAs in health and disease. Cell *152*, 1308–1323.

42. Jégu, T., Aeby, E., and Lee, J.T. (2017). The X chromosome in space. Nat. Rev. Genet. *18*, 377–389.

43. Furlan, G., and Rougeulle, C. (2016). Function and evolution of the long noncoding RNA circuitry orchestrating X-chromosome inactivation in mammals. Wiley Interdiscip. Rev. RNA *7*, 702–722.

44. Zhang, H., Zeitz, M.J., Wang, H., Niu, B., Ge, S., Li, W., Cui, J., Wang, G., Qian, G., Higgins, M.J., et al. (2014). Long noncoding RNA-mediated intrachromosomal interactions promote imprinting at the Kcnq1 locus. J. Cell Biol. *204*, 61–75.

45. Kim, T.K., Hemberg, M., Gray, J.M., Costa, A.M., Bear, D.M., Wu, J., Harmin, D.A., Laptewicz, M., Barbara-Haley, K., Kuersten, S., et al. (2010). Widespread transcription at neuronal activity-regulated enhancers. Nature *465*, 182–187.

46. Andersson, R., Gebhard, C., Miguel-Escalada, I., Hoof, I., Bornholdt, J., Boyd, M., Chen, Y., Zhao, X., Schmidl, C., Suzuki, T., et al. (2014). An atlas of active enhancers across human cell types and tissues. Nature *507*, 455–461.

47. Lai, F., Orom, U.A., Cesaroni, M., Beringer, M., Taatjes, D.J., Blobel, G.A., and Shiekhattar, R. (2013). Activating RNAs associate with Mediator to enhance chromatin architecture and transcription. Nature *494*, 497–501.

48. Cheng, J.H., Pan, D.Z., Tsai, Z.T., and Tsai, H.K. (2015). Genome-wide analysis of enhancer RNA in gene regulation across 12 mouse tissues. Sci. Rep. *5*, 12648.

49. Prabhu, V.V., Siddikuzzaman, Grace, V.M., and Guruvayoorappan, C. (2012). Targeting tumor metastasis by regulating Nm23 gene expression. Asian Pac. J. Cancer Prev. *13*, 3539–3548.

50. Kim, H.D., Youn, B., Kim, T.S., Kim, S.H., Shin, H.S., and Kim, J. (2009). Regulators affecting the metastasis suppressor activity of Nm23-H1. Mol. Cell. Biochem. *329*, 167–173.

51. Marino, N., Nakayama, J., Collins, J.W., and Steeg, P.S. (2012). Insights into the biology and prevention of tumor metastasis provided by the Nm23 metastasis suppressor gene. Cancer Metastasis Rev. *31*, 593–603.

52. Jung, H., Seong, H.A., and Ha, H. (2007). NM23-H1 tumor suppressor and its interacting partner STRAP activate p53 function. J. Biol. Chem. *282*, 35293–35307.

53. Horak, C.E., Lee, J.H., Elkahloun, A.G., Boissan, M., Dumont, S., Maga, T.K., Arnaud-Dabernat, S., Palmieri, D., Stetler-Stevenson, W.G., Lacombe, M.L., et al. (2007). Nm23-H1 suppresses tumor cell motility by down-regulating the lysophosphatidic acid receptor EDG2. Cancer Res. *67*, 7238–7246.

54. Kim, K.H., Yeo, S.G., Yoo, B.C., and Myung, J.K. (2017). Identification of calgranulin B interacting proteins and network analysis in gastrointestinal cancer cells. PLoS ONE *12*, e0171232.

55. Hu, J.F., Vu, T.H., and Hoffman, A.R. (1997). Genomic deletion of an imprint maintenance element abolishes imprinting of both insulin-like growth factor II and H19. J. Biol. Chem. *272*, 20715–20720.

56. Zhao, X., Liu, X., Wang, G., Wen, X., Zhang, X., Hoffman, A.R., Li, W., Hu, J.F., and Cui, J. (2016). Loss of insulin-like growth factor II imprinting is a hallmark associated with enhanced chemo/radiotherapy resistance in cancer stem cells. Oncotarget *7*, 51349–51364.

57. Han, W., Li, W., Zhang, X., Du, Z., Liu, X., Zhao, X., Wen, X., Wang, G., Hu, J.F., and Cui, J. (2017). Targeted breast cancer therapy by harnessing the inherent blood group antigen immune system. Oncotarget *8*, 15034–15046.

58. Yin, H., Chen, N., Guo, R., Wang, H., Li, W., Wang, G., Cui, J., Jin, H., and Hu, J.F. (2015). Antitumor potential of a synthetic interferon-alpha/PLGF-2 positive charge peptide hybrid molecule in pancreatic cancer cells. Sci. Rep. *5*, 16975.

59. Yu, D., Du, Z., Li, W., Chen, H., Ye, S., Hoffman, A.R., Cui, J., and Hu, J.F. (2017). Targeting Jurkat T lymphocyte leukemia cells by an engineered interferon-alpha hybrid molecule. Cell. Physiol. Biochem. *42*, 519–529.

60. Song, W., Li, W., Li, L., Zhang, S., Yan, X., Wen, X., Zhang, X., Tian, H., Li, A., Hu, J.F., and Cui, J. (2015). Friend leukemia virus integration 1 activates the Rho GTPase pathway and is associated with metastasis in breast cancer. Oncotarget *6*, 23764–23775.

61. Wang, H., Chao, K., Ng, S.C., Bai, A.H., Yu, Q., Yu, J., Li, M., Cui, Y., Chen, M., Hu, J.F., and Zhang, S. (2016). Pro-inflammatory miR-223 mediates the cross-talk between the IL23 pathway and the intestinal barrier in inflammatory bowel disease. Genome Biol. *17*, 58.

62. Wang, H., Li, W., Guo, R., Sun, J., Cui, J., Wang, G., Hoffman, A.R., and Hu, J.F. (2014). An intragenic long noncoding RNA interacts epigenetically with the RUNX1 promoter and enhancer chromatin DNA in hematopoietic malignancies. Int. J. Cancer *135*, 2783–2794.

63. Langmead, B., and Salzberg, S.L. (2012). Fast gapped-read alignment with Bowtie 2. Nat. Methods *9*, 357–359.

64. Harrow, J., Frankish, A., Gonzalez, J.M., Tapanari, E., Diekhans, M., Kokocinski, F., Aken, B.L., Barrell, D., Zadissa, A., Searle, S., et al. (2012). GENCODE: the reference human genome annotation for The ENCODE Project. Genome Res. *22*, 1760–1774.

65. Thorvaldsdóttir, H., Robinson, J.T., and Mesirov, J.P. (2013). Integrative Genomics Viewer (IGV): high-performance genomics data visualization and exploration. Brief. Bioinform. *14*, 178–192.

66. Robinson, J.T., Thorvaldsdóttir, H., Winckler, W., Guttman, M., Lander, E.S., Getz, G., and Mesirov, J.P. (2011). Integrative genomics viewer. Nat. Biotechnol. *29*, 24–26.

67. Subramanian, A., Tamayo, P., Mootha, V.K., Mukherjee, S., Ebert, B.L., Gillette, M.A., Paulovich, A., Pomeroy, S.L., Golub, T.R., Lander, E.S., and Mesirov, J.P. (2005). Gene set enrichment analysis: a knowledge-based approach for interpreting genome-wide expression profiles. Proc. Natl. Acad. Sci. USA *102*, 15545–15550.

68. Zhang, S., Zhong, B., Chen, M., Yang, L., Yang, G., Li, Y., Wang, H., Wang, G., Li, W., Cui, J., et al. (2014). Epigenetic reprogramming reverses the malignant epigenotype of the MMP/TIMP axis genes in tumor cells. Int. J. Cancer *134*, 1583–1594.

69. Zhai, Y., Chen, X., Yu, D., Li, T., Cui, J., Wang, G., Hu, J.F., and Li, W. (2015). Histone deacetylase inhibitor valproic acid promotes the induction of pluripotency in mouse fibroblasts by suppressing reprogramming-induced senescence stress. Exp. Cell Res. *337*, 61–67.

70. Li, L., Song, W., Yan, X., Li, A., Zhang, X., Li, W., Wen, X., Zhou, L., Yu, D., Hu, J.F., and Cui, J. (2017). Friend leukemia virus integration 1 promotes tumorigenesis of small cell lung cancer cells by activating the miR-17-92 pathway. Oncotarget *8*, 41975–41987.

71. Wang, L., Guo, H., Lin, C., Yang, L., and Wang, X. (2014). Enrichment and characterization of cancer stem-like cells from a cervical cancer cell line. Mol. Med. Rep. *9*, 2117–2123.

OMTN, Volume *12*

Supplemental Information

Targeting the *IGF1R* Pathway in Breast Cancer Using Antisense lncRNA-Mediated Promoter *cis* Competition

Lingling Pian, Xue Wen, Lihua Kang, Zhaozhi Li, Yuanyuan Nie, Zhonghua Du, Dehai Yu, Lei Zhou, Lin Jia, Naifei Chen, Dan Li, Songling Zhang, Wei Li, Andrew R. Hoffman, Jingnan Sun, Jiuwei Cui, and Ji-Fan Hu

Table S1. Oligonucleotide primers used for PCR

ID	Oligo Name	Oligo sequence	Product size
qPCR expression			
IGFIR	JH217	GAAGTCTGGCTCCGGAGGAGGGTC	180 bp
	JH218	ATGTGGAGGTAGCCCTCGATCAC	
IRAIN	JH248	CGACACATGGTCCAATCACTGTT	138 bp
	JH249	AGACTCCCCTAGGACTGCCATCT	
NM23	WX011	TTGAGCGTACCTCCATTGCGATC	370 bp
	WX012	TTTGCACTCTCCACAGAATCACT	
B-ACTIN	J880	CAGGTCATCACCATTGGCAATGAGC	135 bp
	J881	CGGATGTCCACGTCACACTTCATGA	
Targeting			
	SJ131	CTGGGGTAGAAAGATGACTGAA	
	JH583	ACGCATTTATTTATTTTGCAACAGC	
DNA methylation			
	SJ996	TYGTAYGTTTTGGGGAATYGGGTTT	204 bp
	SJ997	ACTAATAAACAAAAACCCCAACCTC	
	SJ998	GTGTTTTGGATTTGGGAAGGAGTT	279 bp
	SJ999	AAACAAAACCCAAATCTACCTAAAC	
Targeting vector			
	JH1094	CAGTGCAGGGGAAAGAATAG	422 bp
	JH485	TCAGTTTTTAGCCGGGAAGGT	
	SJ130	ACGCGTATATCTGGCCCGTACA	921 bp
	SJ131	CTGGGGTAGAAAGATGACTGAA	
ARM1	SJ016	TCAAAATTTTATCGATATTATCTGGCTATCACTC AGAACCT	777 bp
	SJ017	GCGTATATCTGGCCCGTACATCTTCGAAGATAA GTACGGTTTAGAAGACACG	
PCMV	SJ018	GATGTACGGGCCAGATATACGCG	659 bp
	SJ019	ACCGTGGGCTTGTACTCGGTCATTGTACAATTT CGATAAGCCAGTAAGCAGTG	
PURO	SJ020	ATGACCGAGTACAAGCCCACGGT	612 bp
	SJ021	GCCCTGGGGACGTCGTCGCGGGTGGCGAGGC GCACCGTGGGCTTGTACTCGGTCAT	
ARM2	JH986	GCAGAAGAGAGGGCGACACGACGCCGACCAC AACAAAACCAAGGC	2 kb
	SJ023	TTAAATCGACGCTAGCCCTCGGCTGTGACCTT CAGCGAGC	
PH1-1	SU47	CAGCCGAGGGCTAGCTTTAAGACCAATGACTT ACAAGGC	361 bp
	SJ138	CTAAACGTCTGGTAAGAAATGGGATCCAAGTG GTCTCATACAG	
gRNA1	SJ139	CCCATTTCTTACCAGACGTTTAGTTTTAGAGCT AGAAATAGCAAGTT	140 bp
	SJ140	AGGCCCTCTTCCTGCCCGACCTTGTCGACAAA AAAAGCACCGACTCGGTGCCA	

PU6	SJ141	GTGGCACCGAGTCGGTGCTTTTTTTGTCGACA AGGTCGGGCAGGAAGAGGGCCT	316 bp
	SJ142	CAGTGGGACGCGGACTGGGGCGGTGTTTCGT CCTTTCCACAAGA	
gRNA2	SJ143	CCGCCCCAGTCCGCGTCCCACTGTTTTAGAGC TAGAAATAGCAAGTT	119 bp
	SJ144	GCAAAAAGCAGAATCGAAGAATTCAAAAAAA GCACCGACTCGGTGCCAC	
	SU48	CCCCTACCCATTTAAATGAAGCAAAAAGCAGA ATCGAAGAATTC	
PH1-2	SU47	CAGCCGAGGGCTAGCTTTAAGACCAATGACTT ACAAGGC	361 bp
	SJ145	CTTACTAAGTCGTTTAGGTGGGGATCCAAGTG GTCTCATACAG	
PU6-1	SJ141	GTGGCACCGAGTCGGTGCTTTTTTTGTCGACA AGGTCGGGCAGGAAGAGGGCCT	316 bp
	SJ147	CGACCTTCCACAGATCTGGGCGGTGTTTCGTC CTTTCCACAAGA	
gRNA3	SJ146	CCCCACCTAAACGACTTAGTAAGTTTTAGAGC TAGAAATAGCAAGTT	145 bp
	SJ140	AGGCCCTCTTCCTGCCCGACCTTGTCGACAAA AAAAGCACCGACTCGGTGCCA	
PU6-2	SJ141	GTGGCACCGAGTCGGTGCTTTTTTTGTCGACA AGGTCGGGCAGGAAGAGGGCCT	316 bp
	SJ147	CGACCTTCCACAGATCTGGGCGGTGTTTCGTC CTTTCCACAAGA	
gRNA4	SJ148	CCGCCCAGATCTGTGGAAGGTCGTTTTAGAGC TAGAAATAGCAAGTT	119 bp
	SJ144	GCAAAAAGCAGAATCGAAGAATTCAAAAAAA GCACCGACTCGGTGCCAC	
RAT primers			
	JH513	CCTTTGTCCATGTGGTCAAGTT	
	JH400	CATCAGGTCCCTTCTACCATCC	
	JH745	ACGCATTTATTTATTTTGCAACAGCTGC	
	JH780	GTTTCCGCAGTAGCCGCTGAT	
siRNAs			
	IRAIN1	CCUCAUGCAGAGAACUUAATT	
		UUAAGUUCUCUGCAUGAGGTT	
	IRAIN2	CCAGUCACUUACGUAGCAATT	
		UUGCUACGUAAGUGACUGGTT	
	IRAIN3	CCGCAUGCACGCAUUUAUUTT	
		AAUAAAUGCGUGCAUGCGGTT	
	siCT	UUCUCCGAACGUGUCACGUTT	
		ACGUGACACGUUCGGAGAATT	

SUPPLEMENTARY FIGURE LEGENDS

Figure S1. ALIC targeting of the *IGF1R* and *IRAIN* locus.

A. CRISPR Cas9 *IRAIN*-gRNA targeting vector. Cas9: CRISPR Cas9; gRNA: Cas9 guiding RNAs that target the *IRAIN* promoter (sequences under the diagram); pEF1: the human EF-1a promoter; pH1: human H1 promoter; pU6: U6 promoter; T5: the TTTTT termination signal of RNA polymerase III.

B. Location of the four *IRAIN* Cas9 gRNAs. The *IRAIN* arm fragments was presented in green capitals. The *IRAIN* gRNA sequences were highlighted in yellow and PAM (NGG) in red in the *IRAIN* promoter region.

C. The *IRAIN* donor vector. pCMV: CMV promoter to transcribe the puromycin selection marker gene; pPGK: PGK promoter to transcribe the TK negative selection marker gene; TK+: the herpesvirus thymidine kinase gene for negative selection of the targeting clone cells; loxP: the locus of X-over P1 recombination site recognized by Cre to remove the Puro+ gene; Arm1, Arm2: the *IRAIN* arm sequences used for recombination.

Figure S2. Mapping of the IGF1R targeting locus by DNA sequencing.

A. The *IGF1R-IRAIN* targeting locus. The donor vector contains the IRAIN Arm2-Puro-pCMV-Arm1 insert. The Arm2-Arm1 fragments provide the donor sequences for homologous recombination after the Cas9-induced DNA break. Puro+: Puromycin selection marker used for selection. pCMV: CMV promoter. After homologous recombination and Cre recombinase treatment, the CMV promoter is inserted in front of the *IRAIN* lncRNA. Primers (SJ131 and JH583)

were used to amply the whole targeting locus containing the 5' flanking genomic DNA-Arm2-pCMV-Arm1-3' flanking genomic DNA. The PCR DNA was cloned into a pJet vector for sequencing.

B. Sequencing of the recombination sites in the *IGF1R* locus. The DNA fragment covering the whole targeting locus was sequenced. The joint sites of recombination were marked by red arrows.

Figure S3. IRAIN siRNA knockdown in ALIC targeted cells.

The pCMV-IRAIN knockin cells (ALIC) were transfected with IRAIN siRNAs (siIRAIN) or control siRNA (siCT). Cells were collected for gene analysis of *IRAIN* by quantitative PCR. Error bars represent the standard error of the average of three independent PCR reactions. a,b: $p<0.05$ as compared with the vector control (CTL); c: $p<0.05$ as compared with the siCT control.

Figure S4. The RAT-Seq assay.

Schematic diagram of the nuclear *in situ* lncRNA reverse transcription-associated trap (RAT) assay. After crosslinking to fix the lncRNA-chromatin structure, *IRAIN* lncRNA was *in situ* reverse transcribed into lncDNA in the nucleus with biotin-dCTP. The *IRAIN*-binding chromatin DNAs were sonicated into fragments and purified with streptavidin breads. After reversal of crosslink, lncDNA was extracted for DNA library construction and Illumina sequencing.

Figure S5. The *IRAIN* lncRNA binding targets.

Gene ontology analysis of *IRAIN* target genes from the nuclear *in situ* lncRNA reverse transcription-associated trap (RAT) assay.

Figure S6. Expression of target genes and cell growth in *IRAIN*-overexpressing cells.

A. MDA-MB-231 tumor cells were infected with lentiviruses carrying the 5K *IRAIN* cDNA (IRAIN5K) or the copGFP vector control (Vector). After viral infection, cells were selected by puromycin and were collected for gene analysis of *IRAIN* target genes using quantitative PCR. The data shown are mean ± SD of three independent PCR reactions. * $p<0.05$, ** $p<0.01$ as compared with the vector control.

B. Cell proliferation. The *IRAIN*-overexpressing stable cells were collected for analysis of cell proliferation using the MTT assay. The cells that stably expressed the copGFP vector were used as the vector control (Vector). Cell growth was measured as the relative absorbance by setting 0 hour as 1. All experiments were performed in triplicate.

C. Cell cycle. The *IRAIN*-overexpressing stable cells and the vector control cells were collected at 24 hrs, 48 hrs, and 7 hrs for FACS analysis. Cell cycle phase distribution was determined by Cell Quest Pro software and was calculated as the relative value for each phase. No significance of phase distribution was detected between the *IRAIN*-overexpressing and vector control cells.

D. Cell migration. Cell migration was measured by scratch assay at 19 hrs following cell plating.

A. *IGF1R* ALIC gRNA vector

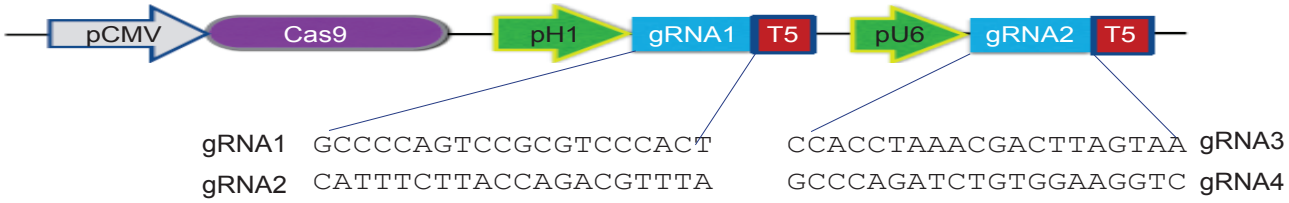

B. Location of Cas9-gRNAs

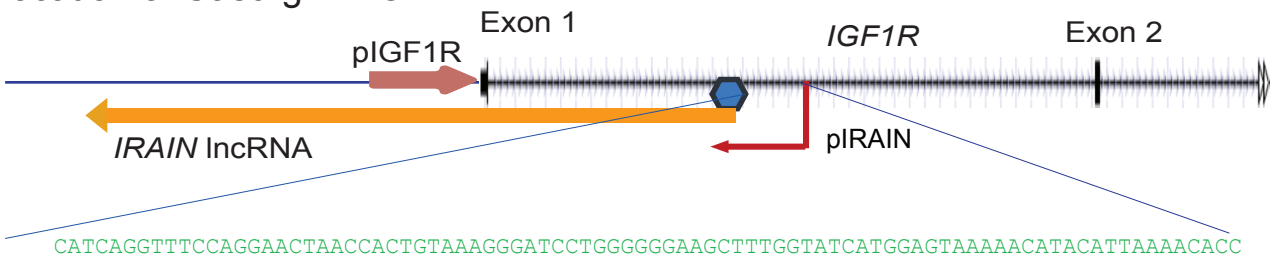

CATCAGGTTTCCAGGAACTAACCACTGTAAAGGGATCCTGGGGGGAAGCTTTGGTATCATGGAGTAAAAACATACATTAAAACACC
CCCTCCCTCCTGCCTGTGTTCTCAAAAATCGCCGTCTTGCACAAAGAATATCCTTCAAGAAGAACGCTCCAAAAGAAAAACAGCCT
ATTTTAAAATGCCCGACTCCTGCGTCGGCGAAGGCCATCCCTGCTGTTTTGAATTTCAGAACATTAAAAACACAAAACTAGAGAAG
CTATACAGTTCAACTGCATAACATAACAAAATGGATTATTTCTCCCGTGTCTTCTAAACCGTACTTATCttttaaagataaaaacc
ctcctttgtccccccagccaCCACCTAAACGACTTAGTAAAGGgagccggaaggctttcgcccaatcgagtccgctgaaagtttag
aaaacaaagagcaggagaGCCCAGATCTGTGGAAGGTCCGGCCCCAGTCCGCGTCCCACTCGGcagtaaacacgcgaaccacgatc
tgctctcgttccgtcgcggactCATTTCTTACCAGACGTTTAAGGatttgtttatagaaaCAGCCTTTCTGAATTGCCCcgGTGAT
GGGGCCATACAACCTCcgCTGCCTCCTCCTTCCCcgCCTCACTCGTGAAGGCTCAGTCGTGATTTTTTCAAAGTTAATCGGCACCA
CCTGCATACCCT

C. Donor vector

Figure S1. *IGF1R* ALIC Cas9-gRNA targeting and donor vectors

A. The *IGF1R-IRAIN* locus

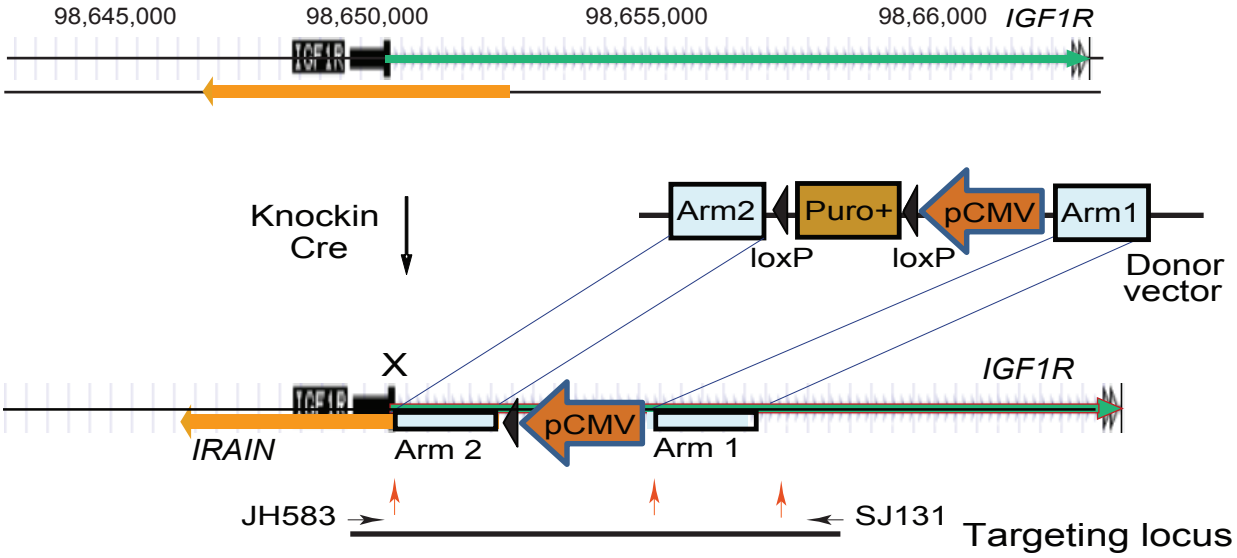

B. Sequencing of the *IGF1R* targeting locus

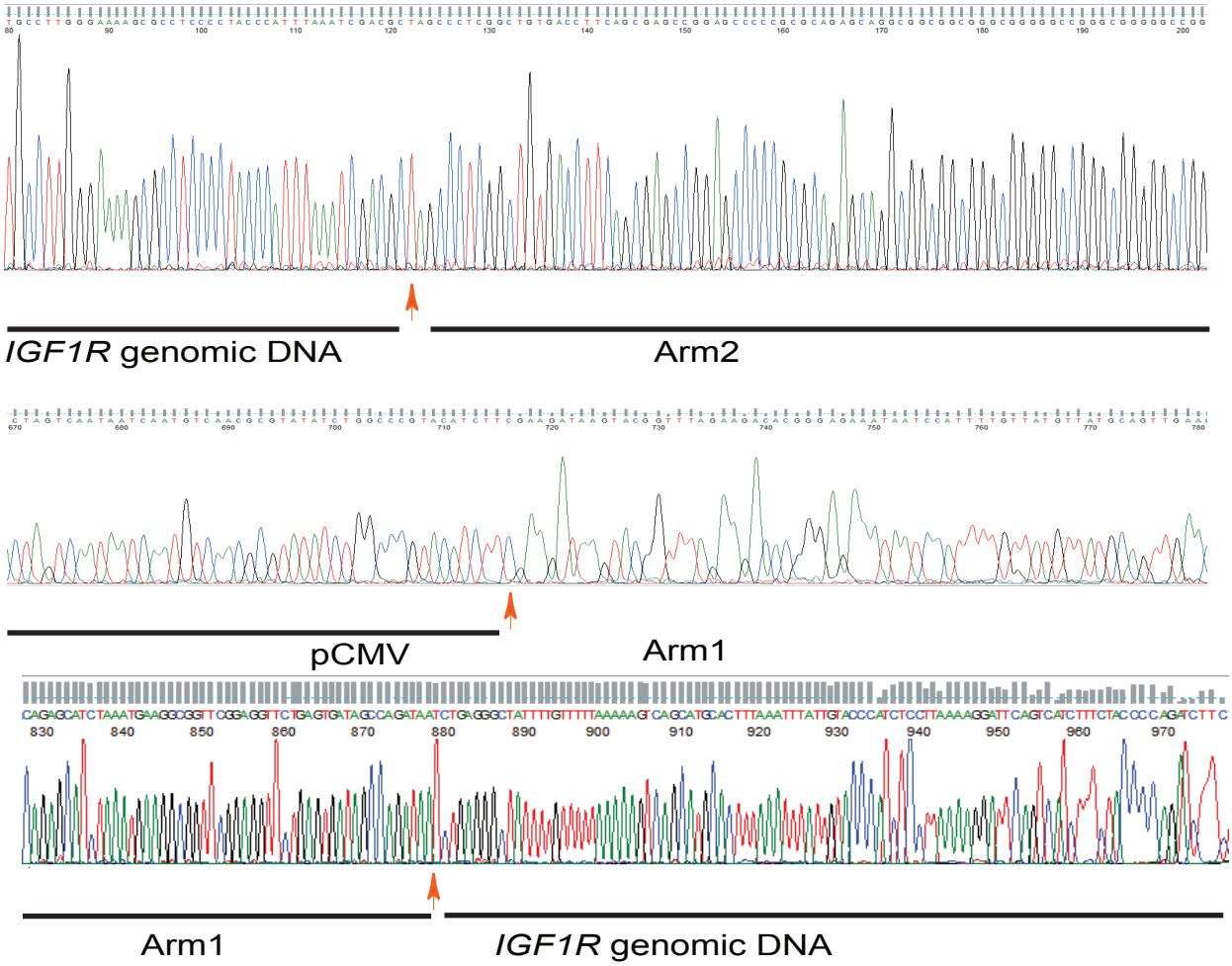

Figure S2. Sequencing of the targeting site of the *IGF1R* locus

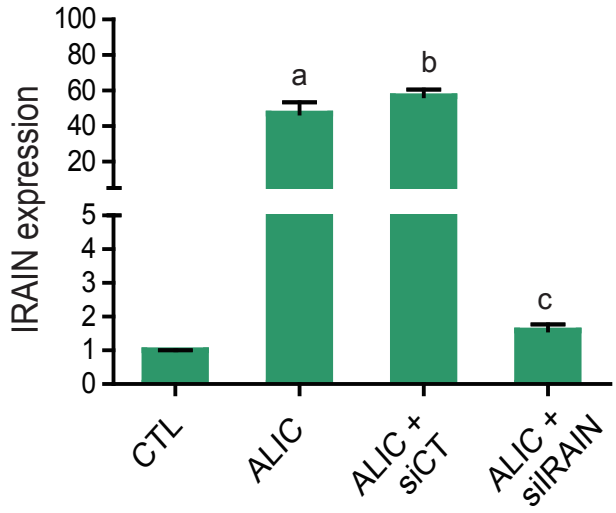

Figure S3. Knockdown of IRAIN lncRNA by siRNAs in ALIC targeted cells

A. Nuclear *in situ* RAT assay

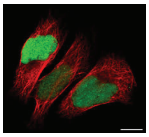

Cell fixation

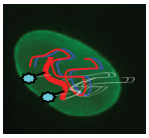

IRAIN lncRNA nulcear *in situ* RT
(biotin-*IRAIN* lncDNA)

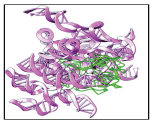

Chromatin sonication

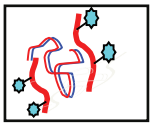

Streptavidin bead purification of *IRAIN* lncDNA
library construction

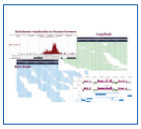

DNA sequencing
IRAIN target analysis

Figure S4. *IRAIN* lncRNA in situ RAT assay

A. *IRAIN* RAT-Seq targets

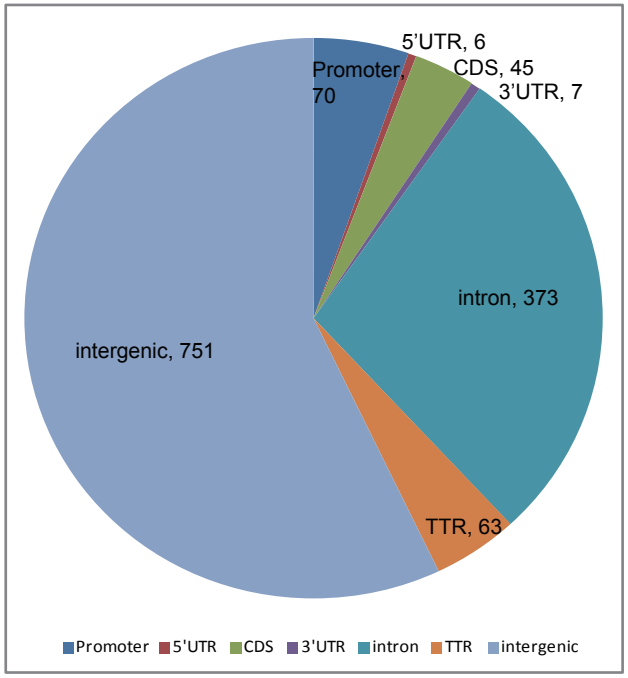

Figure S5. *IRAIN* RAT-Seq targets

A. *IRAIN* target gene expression

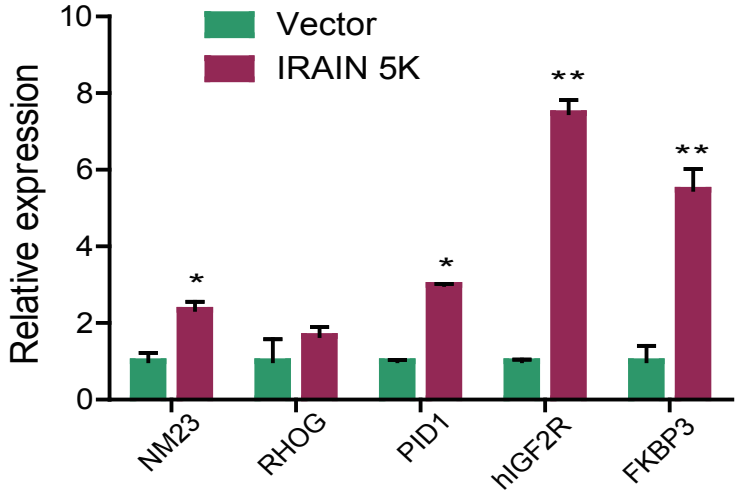

B. Cell proliferation

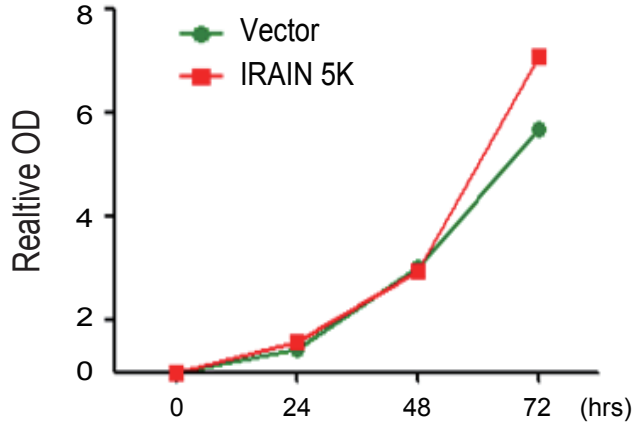

C. Cell cycle

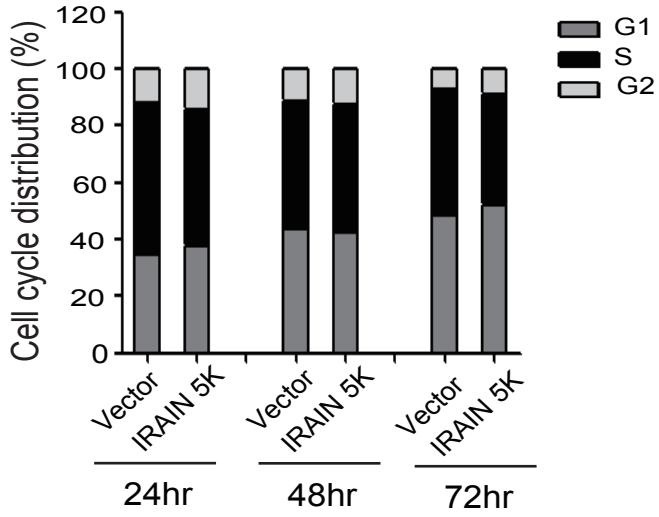

D. Cell migration

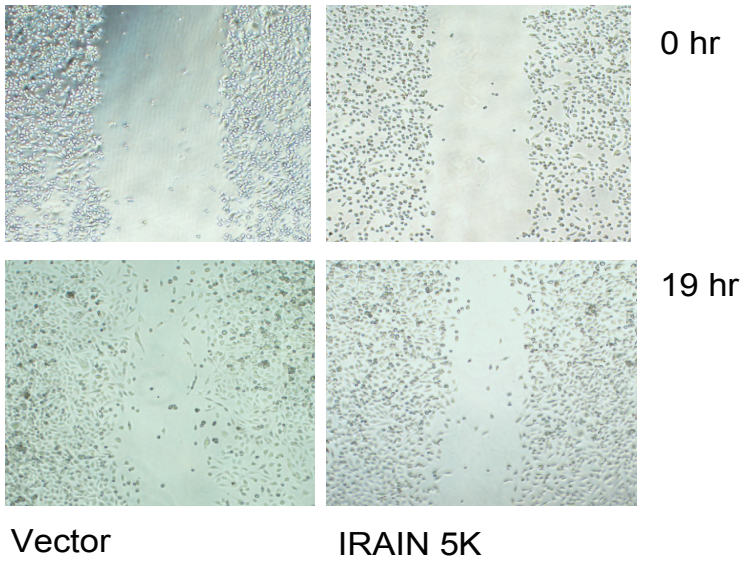

Figure S6. Target genes and cell growth in the *IRAIN trans*-overexpressing cells